Phase-field cohesive zone crack propagation model for hard-soft architected materials

Aimane Najmeddine, Ph.D.
Associate Research Schola

ARCHITECTED MATERIALS AND
ADDITIVE MANUFACTURING LAB

PRINCETON
ENGINEERING

Nacre’s overlapping crystal-protein plates provides toughness

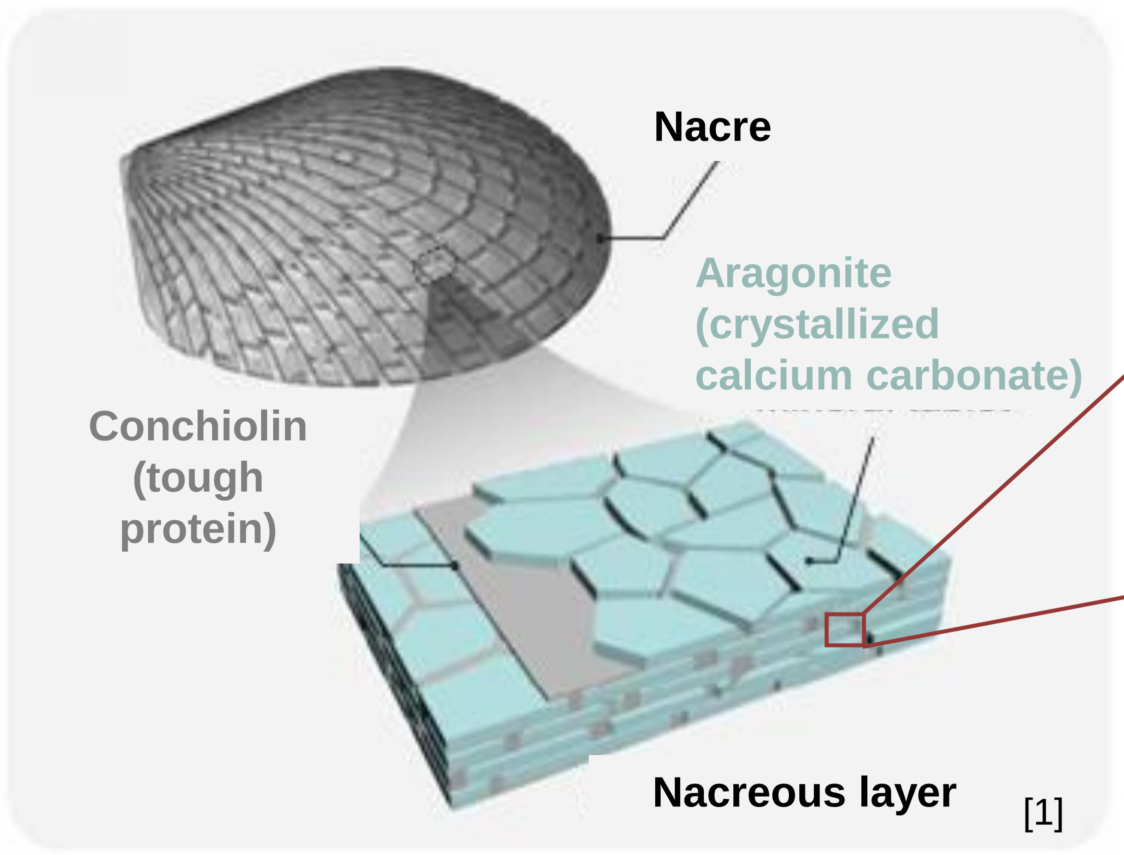

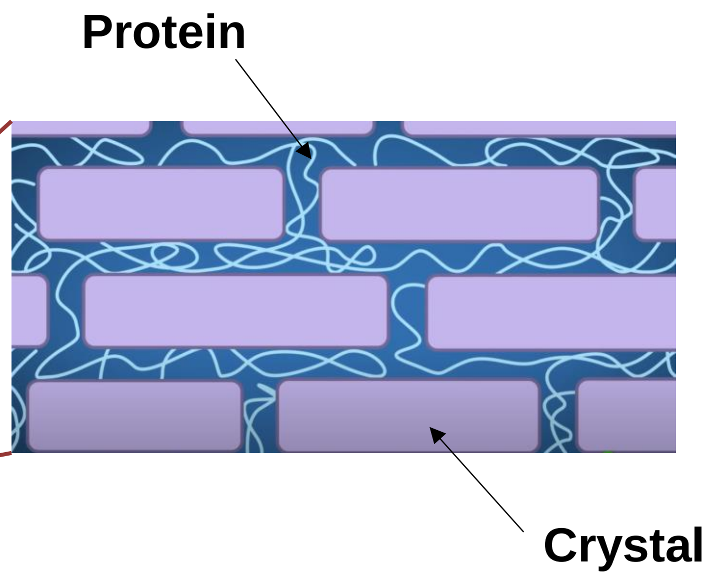

[1] Jin et al., Sci. Adv. 8, eabq3248 (2022)

Hypothesis: hard-soft multi-materials enhance mechanical performance

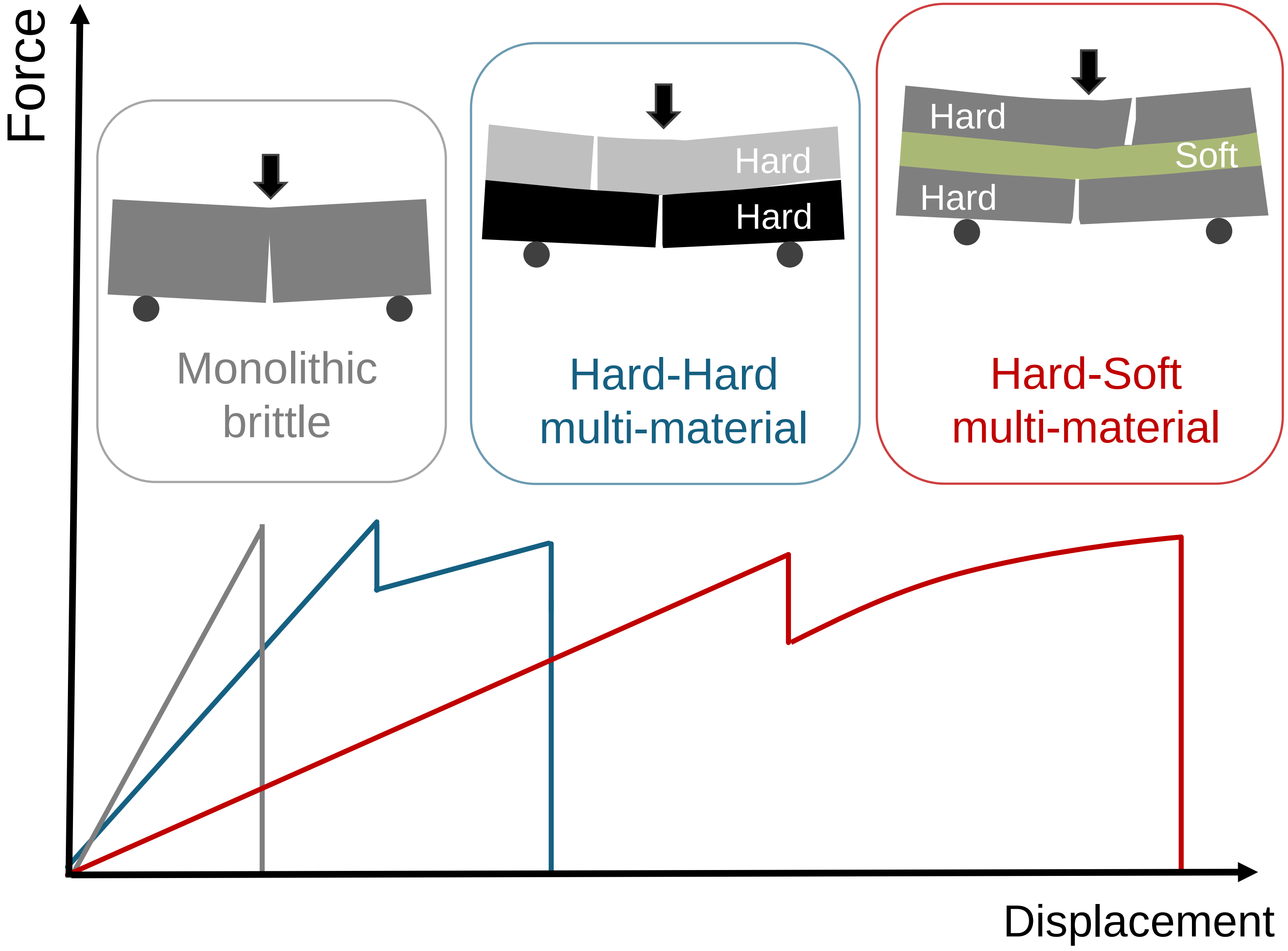

How do we numerically investigate fracture in hard-soft multi-material assemblies to better understand the toughening mechanisms involved in their response to fracture?

How do we numerically investigate fracture in such composite materials?

Phase-field approach for modeling fracture

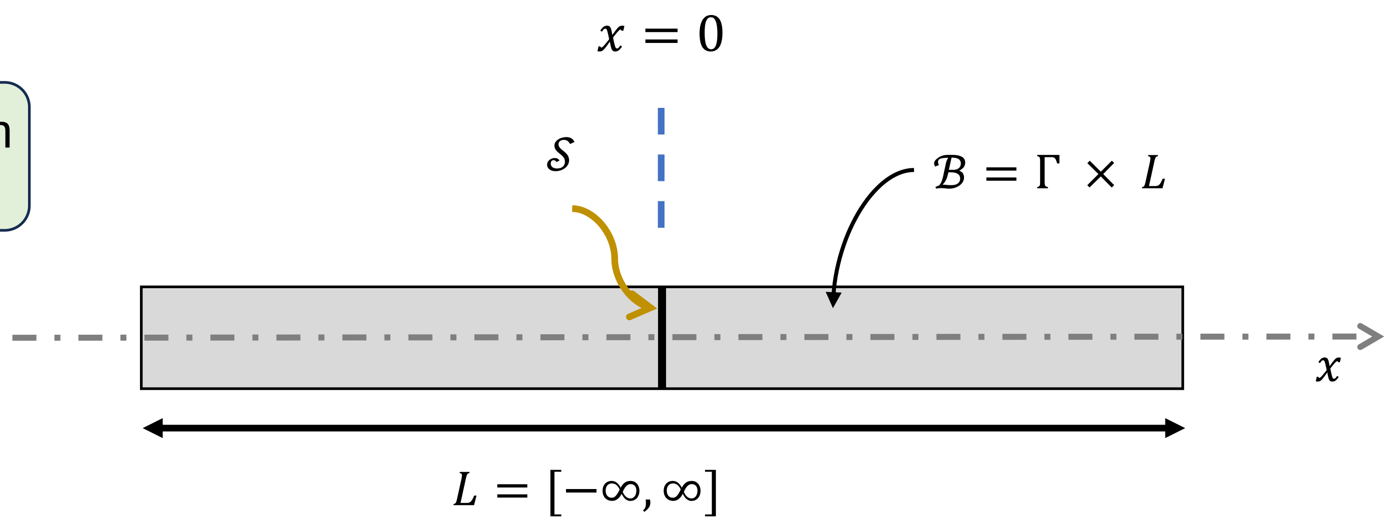

$d \equiv$ auxiliary field variable,
$d \in [0,1]$

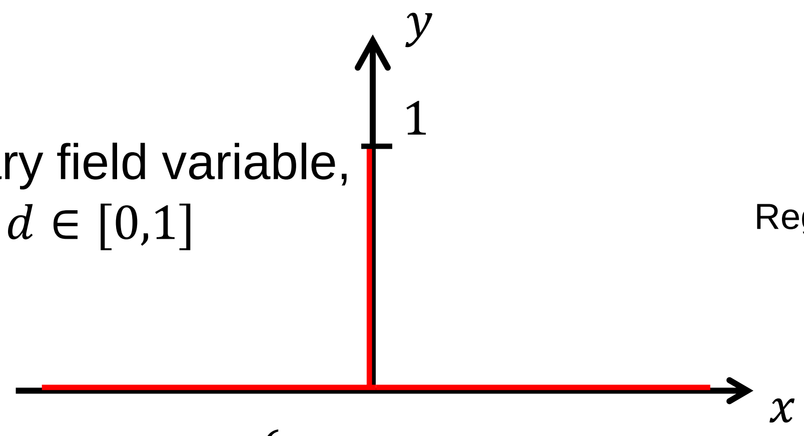

$$d(x) := \begin{cases} 1, & x = 0 \\ 0, & otherwise \end{cases}$$

Regularizing non-smooth sharp crack with a diffuse crack topology

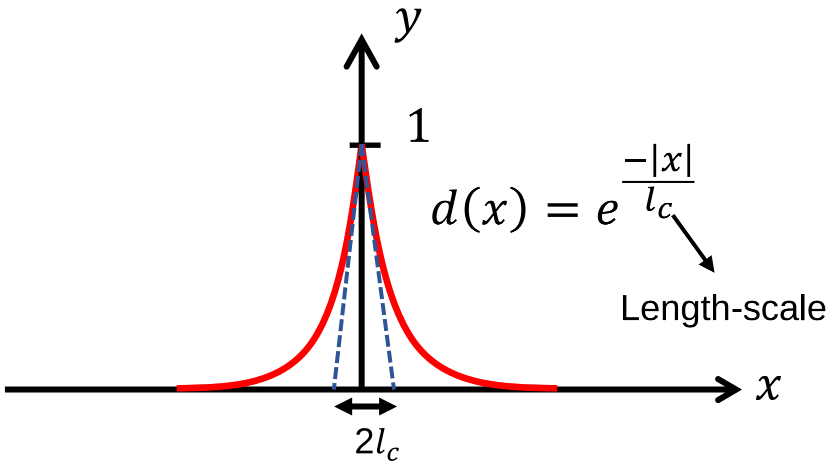

satisfying $\begin{cases} d(0) = 1 \\ d(\pm\infty) = 0 \end{cases}$

Phase-field captures crack propagation through regularization of sharp crack topology

$\mathcal{S}_0$: sharp crack topology
$\mathcal{B}$: diffuse damage band

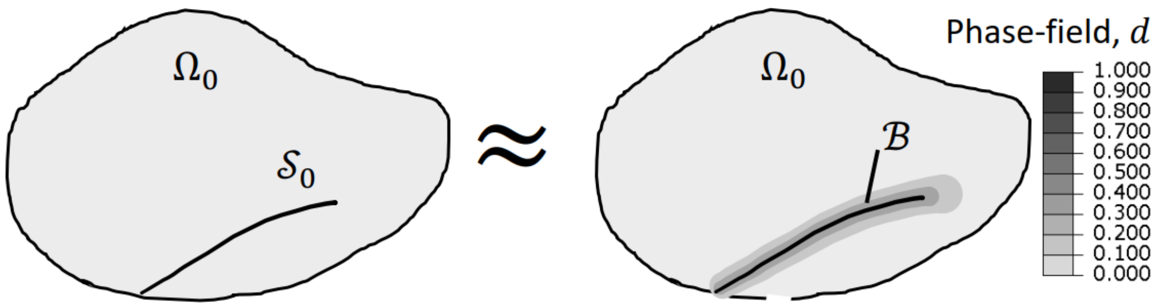

Initial configuration with a sharp crack

Initial configuration with a crack band representation

Regularize the sharp crack topology by a limited diffuse damage band

A time-dependent phase-field damage variable $d(\mathbf{X}, t) \in [0,1]$ is introduced where $d = 0$ indicates no fracture and $d = 1$ indicates complete fracture

Crack surface energy

$$\boxed{\Psi(\mathcal{S}_0) = \int_{\mathcal{S}_0} G_c \, \mathrm{dA} \approx \int_{\Omega_0} G_c \, \gamma(d, \nabla d) \mathrm{d}V}$$

G_c: *Fracture energy* γ: *crack surface density function*

where $$\gamma(d, \nabla d) = \frac{1}{c_\alpha}\left[\frac{1}{l_c}\alpha(d) + l_c |\nabla d|^2\right] \qquad c_\alpha = 4\int_0^1 \sqrt{\alpha(\beta)}\, d\beta = \begin{cases} 2, & \alpha(d) = d^2 \quad \text{AT2} \\ \dfrac{8}{3}, & \alpha(d) = d \quad \text{AT1} \end{cases}$$

l_c: length scale

Phase-field captures crack propagation through regularization of sharp crack topology

Kinematics

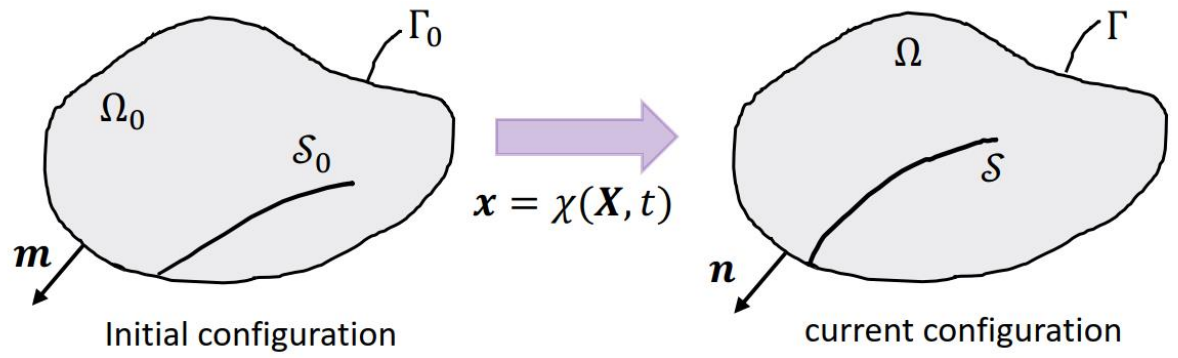

$\mathbf{F} = \nabla\boldsymbol{\chi}(\mathbf{X}, t) = \mathbf{I} + \nabla\mathbf{u}$
deformation gradient

$\mathbf{u}$: displacement field

Total potential energy of the system

$$\underbrace{\Pi(\mathbf{u}, d)}_{\textit{total potential}} = \underbrace{\int_{\Omega_0} g(d)\overset{\text{Strain energy density}}{\psi_0(\mathbf{F})}dV}_{\textit{strain energy}} + \underbrace{\boxed{\int_{\Omega_0} G_c\,\gamma(d, \nabla d)\mathrm{d}V}}_{\textit{crack surface energy}} - \underbrace{\left(\int_{\Omega_0} \overset{\text{Body forces}}{\boldsymbol{b_0}} \cdot \mathbf{u}dV + \int_{\Gamma_0} \overset{\text{Applied traction}}{\mathbf{t_0}} \cdot \mathbf{u}dA\right)}_{\textit{external energy}}$$

Variational principle

$g(d) = (1 - \mathrm{d})^2$: degradation function

$$\big(\mathbf{u}(\mathbf{x}), d(\mathbf{x})\big) = \mathrm{Arg}\{\min \Pi(\mathbf{u}, d)\} \quad \text{subject to } \dot{d}(\mathbf{x}) > 0, d(\mathbf{x}) \in [0,1],\ \mathbf{x} \in \mathbb{R}^n, n = 1,2,3$$

Contribution of interface to the crack surface energy can be accounted for separately

Updated crack surface energy

$$\int_{\Omega_0} G_c^b \gamma(d, \nabla d)\mathrm{d}V + \int_{\Gamma_0} G^i \mathrm{dA}$$

Bulk

Interface

G_c^b: fracture energy of the bulk material

G^i: fracture energy dissipated at the interface

$$\int_{\Gamma_0} G^i \mathrm{dA} = \int_{\Gamma_0} (\Delta\mathbf{u})^{\mathrm{T}} \mathbf{T} \mathrm{dA}$$

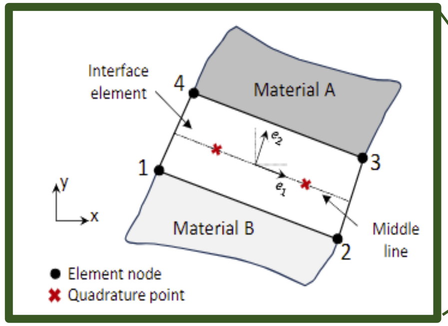

$\Delta\mathbf{u} = \mathbf{u_1} - \mathbf{u_2}$ displacement jump vector

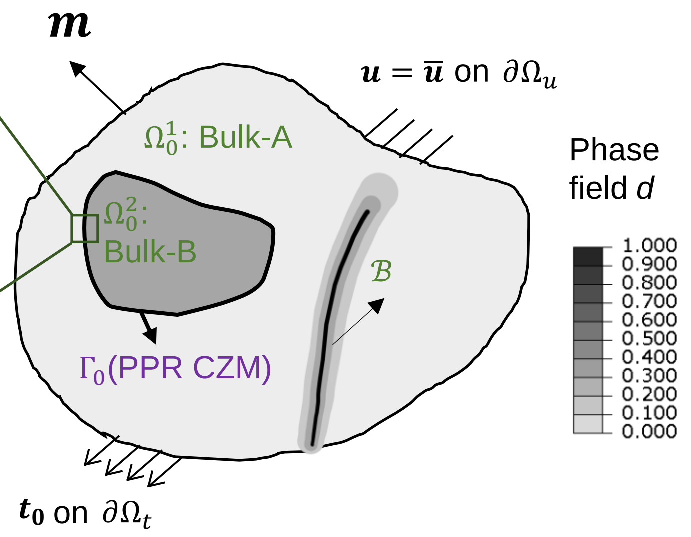

$\mathcal{B}$: smeared crack – modeled by Phase-field

Γ_0: Interface – modeled by PPR CZM

Updated total potential energy of the system

Displacement field

Phase-field

Strain energy density

CZM

Body forces

Applied traction

$$\underbrace{\Pi(\mathbf{u}, d)}_{\textit{total potential}} = \underbrace{\int_{\Omega_0} g(d)\psi_0(\mathbf{F}) dV}_{\textit{strain energy}} + \underbrace{\int_{\Omega_0} G_c^b \gamma(d, \nabla d)\mathrm{d}V + \int_{\Gamma_0} (\Delta\mathbf{u})^{\mathrm{T}}\mathbf{T} \; \mathrm{dA}}_{\textit{crack surface energy}} - \underbrace{\left(\int_{\Omega_0} \boldsymbol{b_0} \cdot \mathbf{u} dV + \int_{\Gamma_0} \mathbf{t_0} \cdot \mathbf{u} dA\right)}_{\textit{external energy}}$$

Bulk

Interface

Park-Paulino-Roesler (PPR) [1] was used to capture dissipated energy at interfacial zones

User-Element Subroutine (UEL) for Abaqus

$$\phi(\Delta\mathbf{u}_n, \Delta\mathbf{u}_t) = \min\left(G_{c\ \ n}^{int}, G_{c\ \ t}^{int}\right) + \left[\Gamma_n\left(1-\frac{\Delta\mathbf{u}_n}{\delta_n}\right)^{\alpha}\left(\frac{m}{\alpha}+\frac{\Delta\mathbf{u}_n}{\delta_n}\right)^{m} + \left\langle \boxed{G_{c\ \ n}^{int}} - \boxed{G_{c\ \ t}^{int}}\right\rangle\right] \text{x} \left[\Gamma_t\left(1-\frac{|\Delta\mathbf{u}_t|}{\delta_t}\right)^{\beta}\left(\frac{n}{\beta}+\frac{|\Delta\mathbf{u}_t|}{\delta_t}\right)^{n} + \left\langle \boxed{G_{c\ \ t}^{int}} - \boxed{G_{c\ \ n}^{int}}\right\rangle\right]$$

$G_{c\ \ n}^{int}, G_{c\ \ t}^{int}$: Energies for mode I and mode II fracture, respectively
Γ_n, Γ_t: Energy constants
$\Delta\mathbf{u}_n, \Delta\mathbf{u}_t$: Normal and tangential components of the displacement jump
δ_n, δ_t: Final crack openings representing complete failure in the normal and tangential directions, respectively
α, β: shape parameters

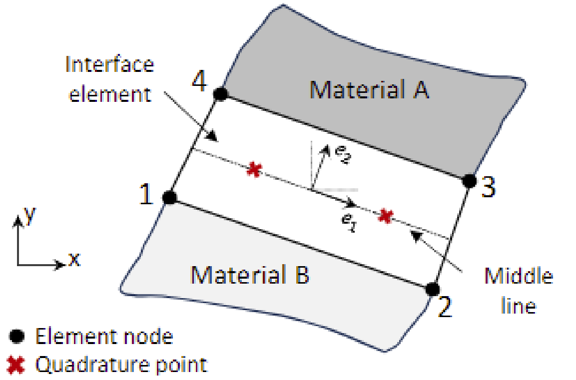

- Normal traction force

$$T_n(\Delta\mathbf{u}_n, \Delta\mathbf{u}_t) = \frac{\Gamma_n}{\delta_n}\left[m\left(1-\frac{\Delta\mathbf{u}_n}{\delta_n}\right)^{\alpha}\left(\frac{m}{\alpha}+\frac{\Delta\mathbf{u}_n}{\delta_n}\right)^{m-1} - \alpha\left(1-\frac{\Delta\mathbf{u}_n}{\delta_n}\right)^{\alpha-1}\left(\frac{m}{\alpha}+\frac{\Delta\mathbf{u}_n}{\delta_n}\right)^{m}\right] \text{x}$$
$$\left[\Gamma_t\left(1-\frac{|\Delta\mathbf{u}_t|}{\delta_t}\right)^{\beta}\left(\frac{n}{\beta}+\frac{|\Delta\mathbf{u}_t|}{\delta_t}\right)^{n} + \left\langle G_{c\ \ t}^{int} - G_{c\ \ n}^{int}\right\rangle\right]$$

$$\boxed{T_n(\delta_{nc}, 0) = \sigma_{max}}$$

- Tangential traction force

$$T_t(\Delta\mathbf{u}_n, \Delta\mathbf{u}_t) = \frac{\Gamma_t}{\delta_t}\left[n\left(1-\frac{|\Delta\mathbf{u}_t|}{\delta_t}\right)^{\beta}\left(\frac{n}{\beta}+\frac{|\Delta\mathbf{u}_t|}{\delta_t}\right)^{n-1} - \beta\left(1-\frac{|\Delta\mathbf{u}_t|}{\delta_t}\right)^{\beta-1}\left(\frac{n}{\beta}+\frac{|\Delta\mathbf{u}_t|}{\delta_t}\right)^{n}\right]$$
$$\text{x}\left[\Gamma_n\left(1-\frac{\Delta\mathbf{u}_n}{\delta_n}\right)^{\alpha}\left(\frac{m}{\alpha}+\frac{\Delta\mathbf{u}_n}{\delta_n}\right)^{m} + \left\langle G_{c\ \ t}^{int} - G_{c\ \ n}^{int}\right\rangle\right]\left(\frac{\Delta\mathbf{u}_t}{|\Delta\mathbf{u}_t|}\right)$$

$$\boxed{T_t(0, \delta_{tc}) = \tau_{max}}$$

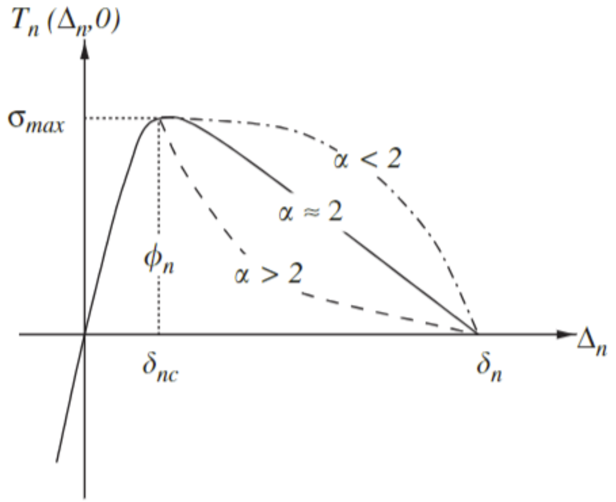

Updated crack surface energy

$$\int_{\Gamma_0} G^i \mathrm{dA} = \int_{\Gamma_0} \boxed{(\Delta\mathbf{u})^{\mathrm{T}}}\ \boxed{\mathbf{T}}\ \mathrm{dA} \quad \text{where} \quad \boxed{\Delta\mathbf{u} = \mathbf{u_1} - \mathbf{u_2}} \quad \text{and} \quad \boxed{\mathbf{T} = (T_n, T_t)}$$

Displacement jump **Traction force vector**

[1] K. Park et al. / J. Mech. Phys. Solids 57 (2009) 891–90

Crack propagation was investigated for four cases of hard-hard and hard-soft composites

Case I: hard-hard bi-layer composite with interface perpendicular to initial notch direction

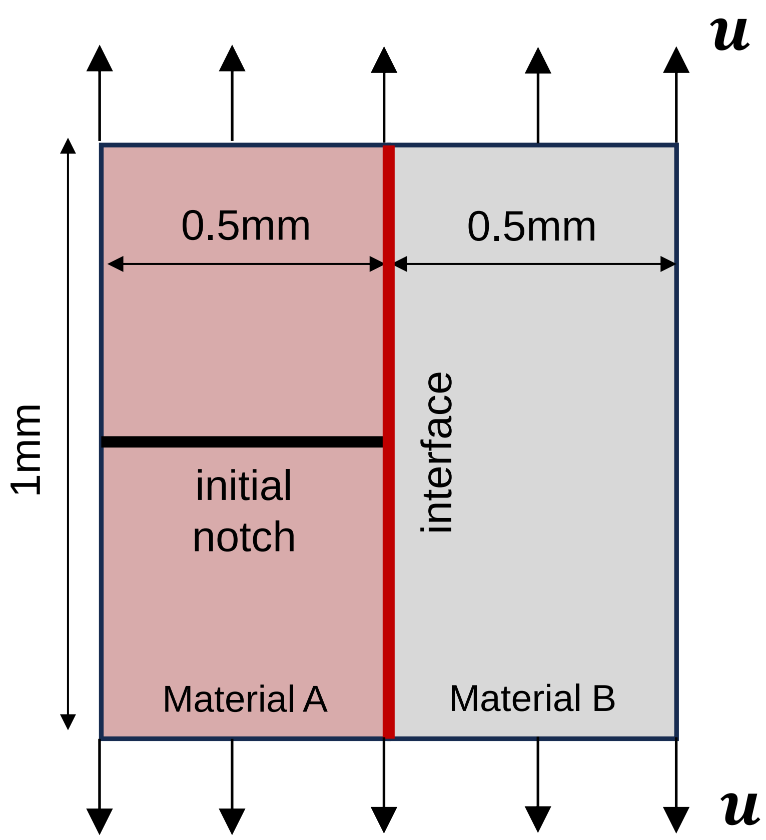

Case II: solid with crack impinging on an incline interface

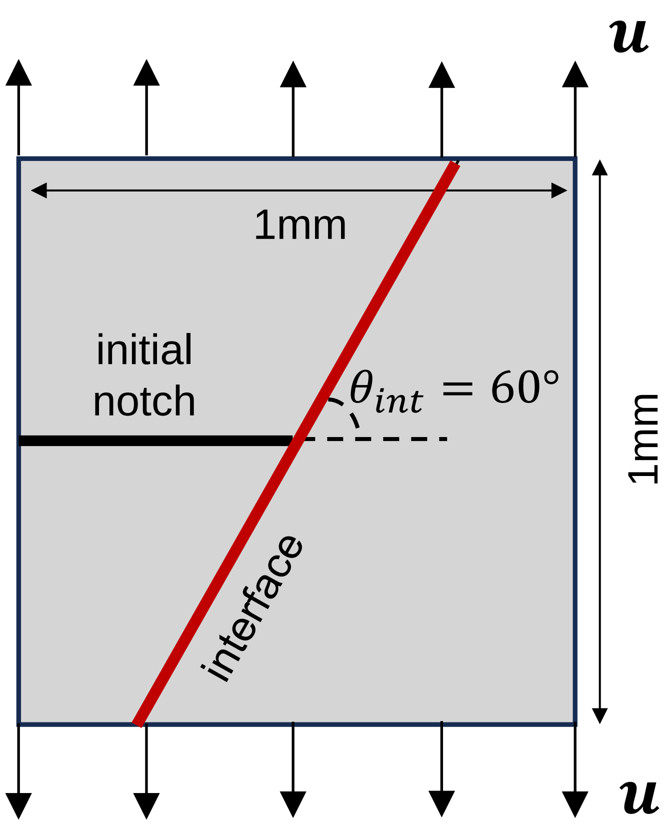

Crack propagation was investigated for four cases of hard-hard and hard-soft composites

Case III: hard-soft-hard tri-layer composite with interface perpendicular to initial notch direction

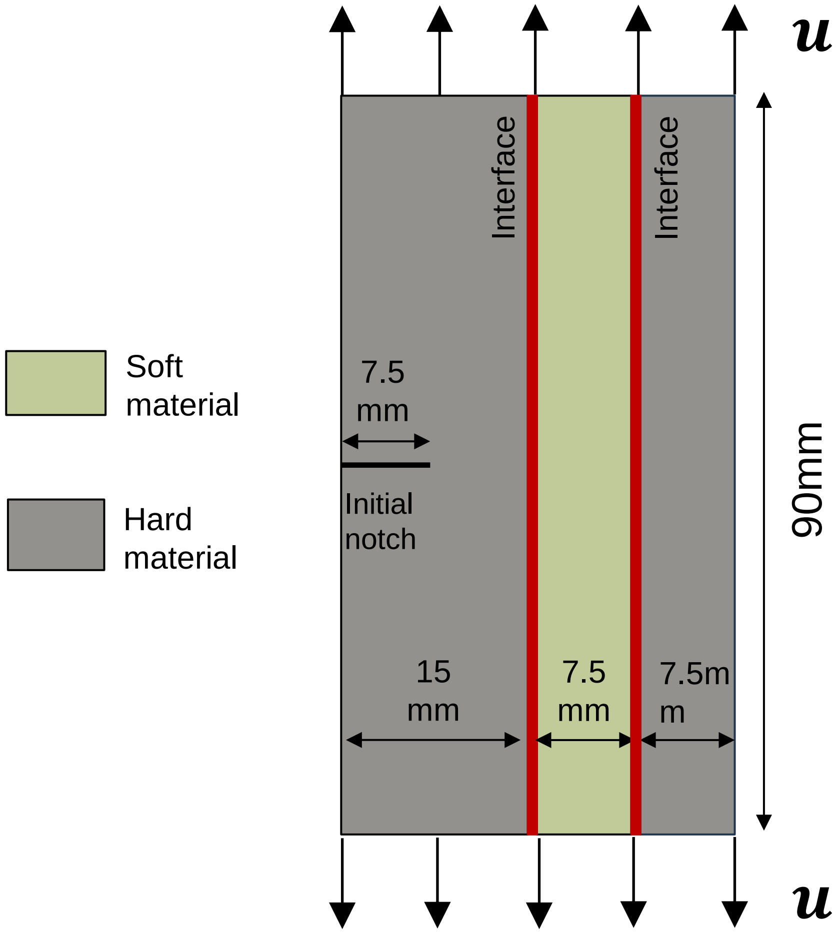

Case IV: fiber-reinforced matrix composite

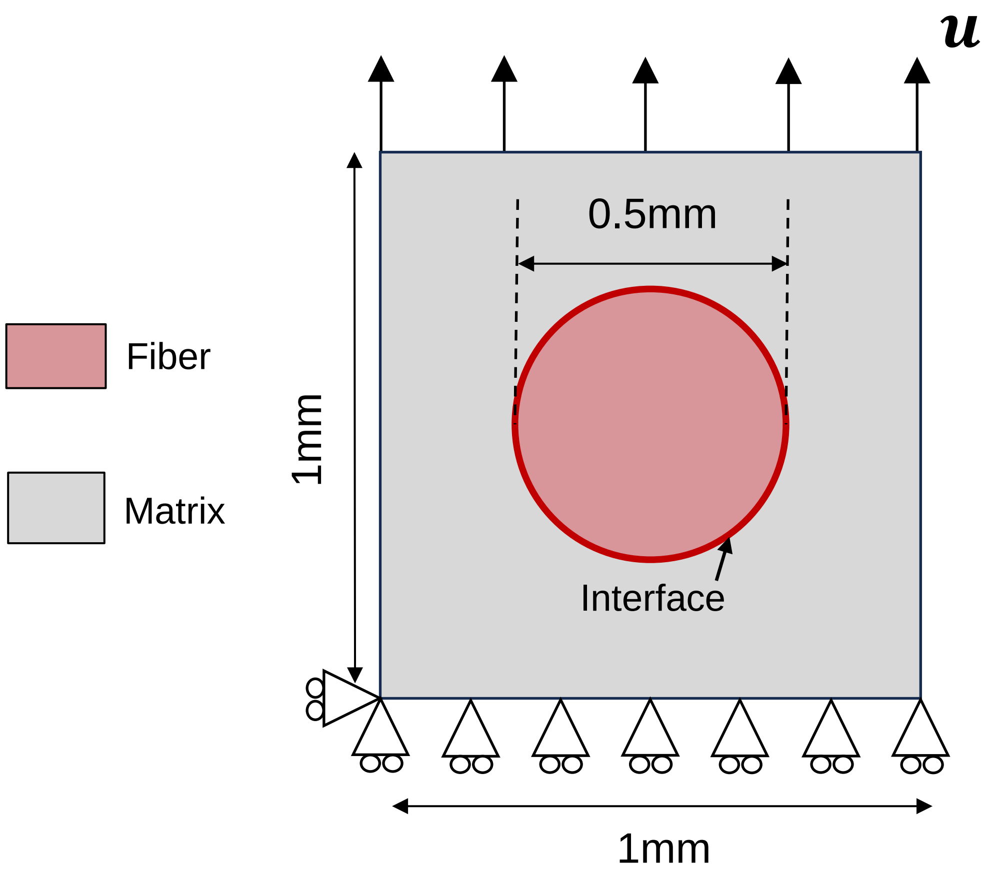

LEFM shows two predominant crack growth mechanisms in hard-hard bi-layer materials

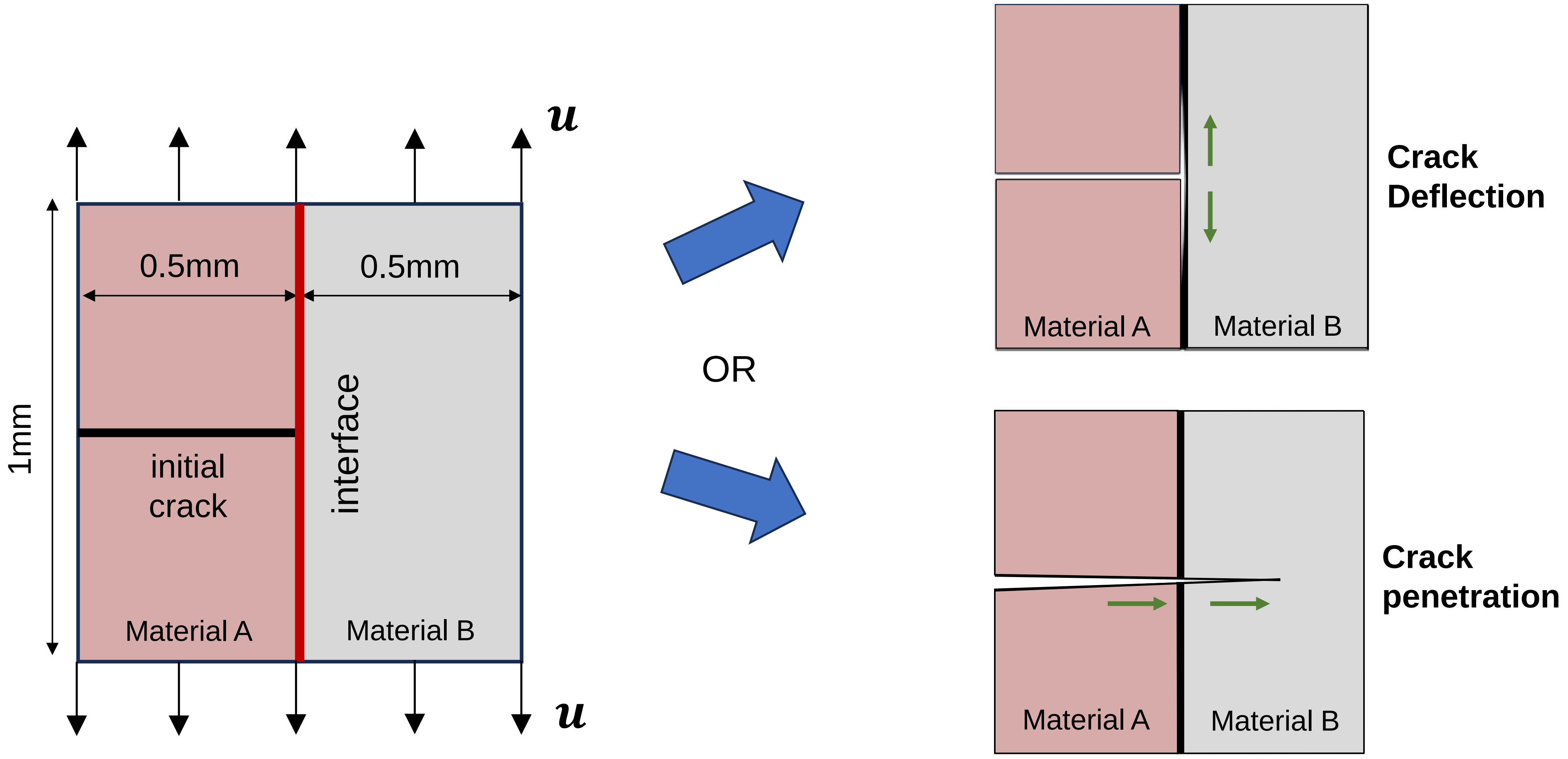

Crack propagation mode depends on material and interfacial fracture properties

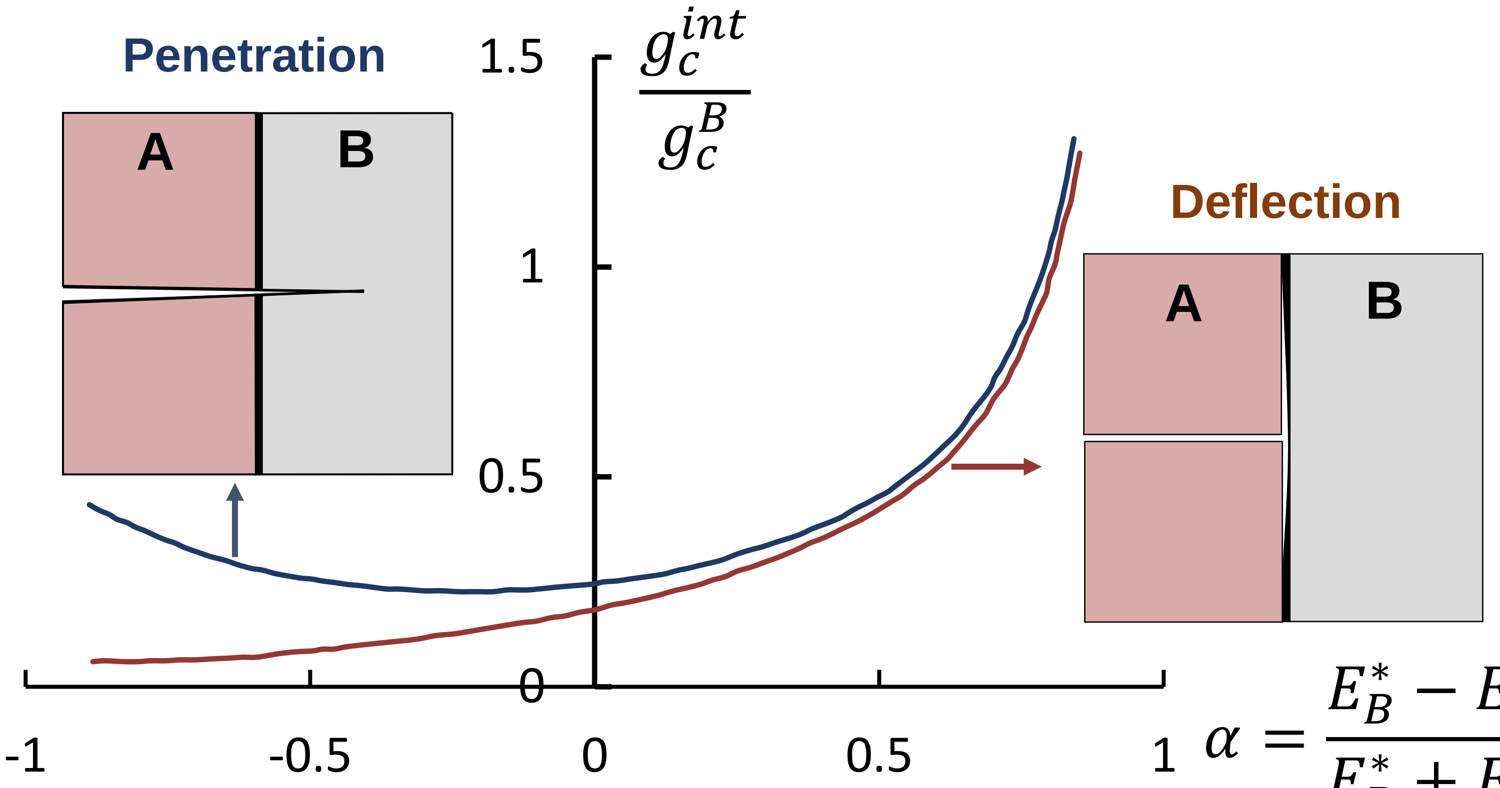

$$\alpha = \frac{E_B^* - E_A^*}{E_B^* + E_A^*}$$

E^*: Plane strain Young's Modulus

α: Parameter characterizing elastic mismatch of bi-material system [1]

$\frac{g_c^{int}}{g_c^B}$: Ratio between the fracture energy of the interface and the fracture energy of bulk Material B [1]

[1] He and Hutchinson / *Int. J. Solids Structures* 29 (1989) 63-191

LEFM shows two predominant crack growth mechanisms in hard-hard bi-layer materials

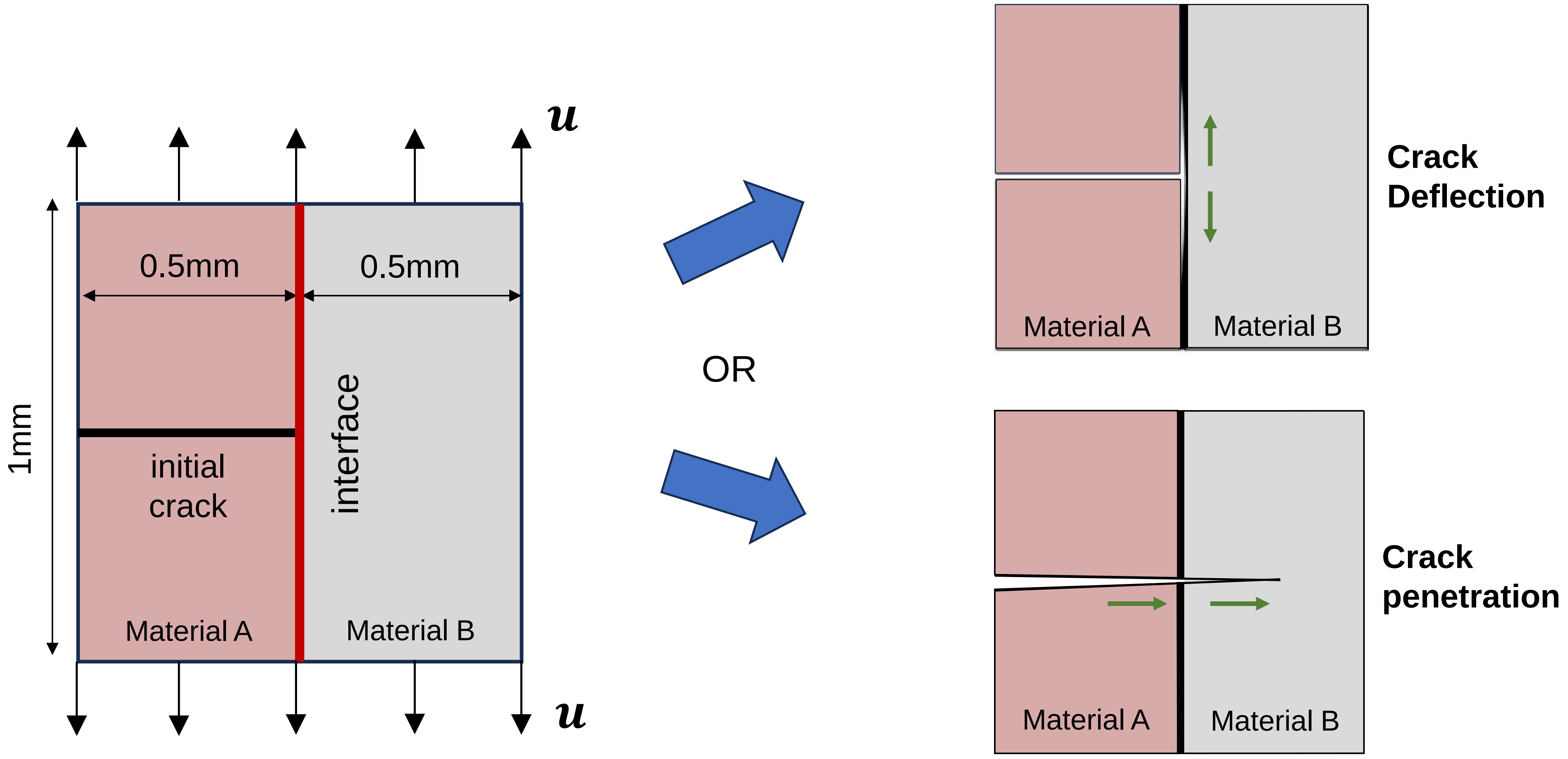

Crack penetration

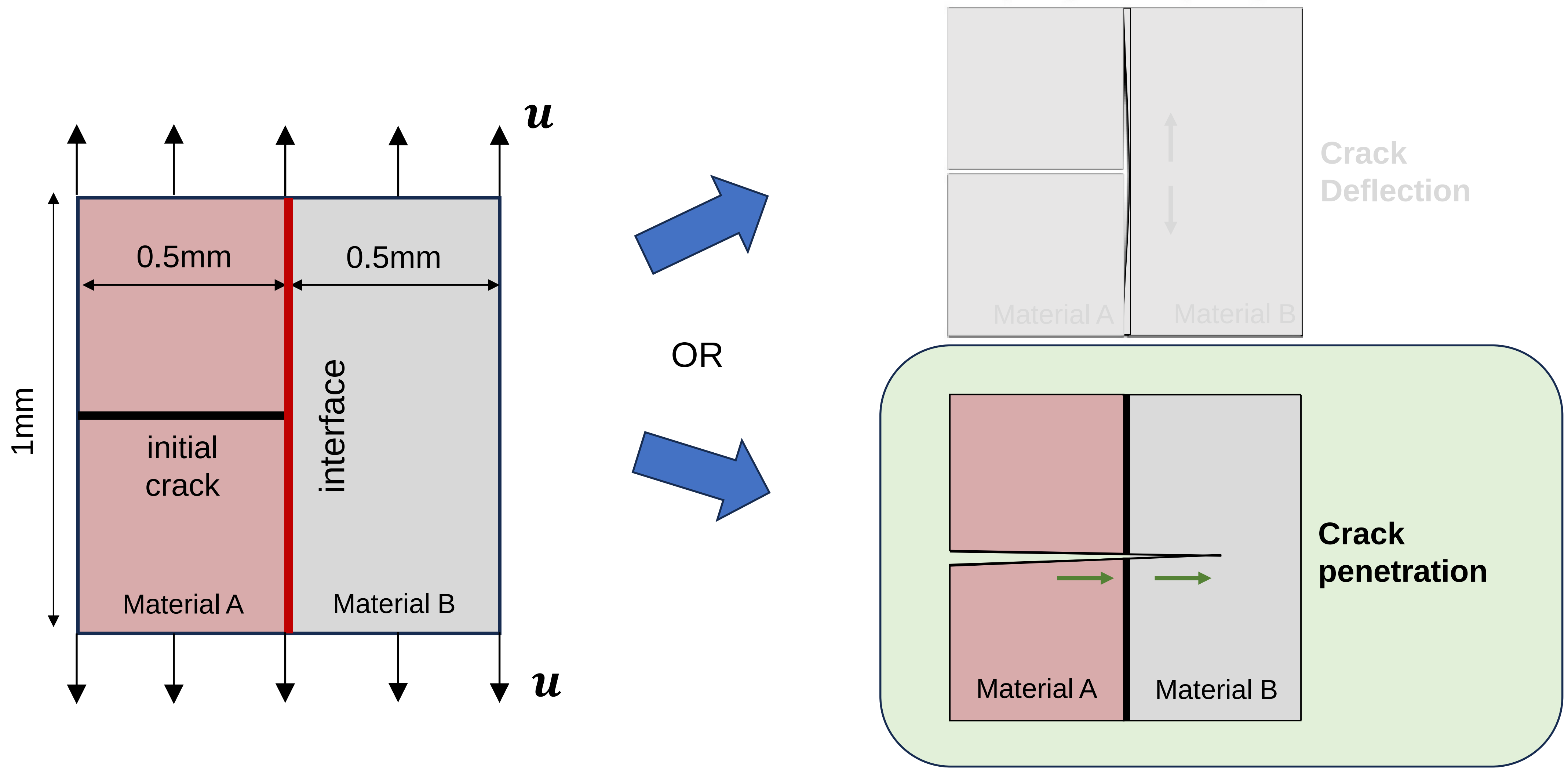

Zero-thickness cohesive elements used for interface - 4-node quadrilateral plane strain elements used for bulk

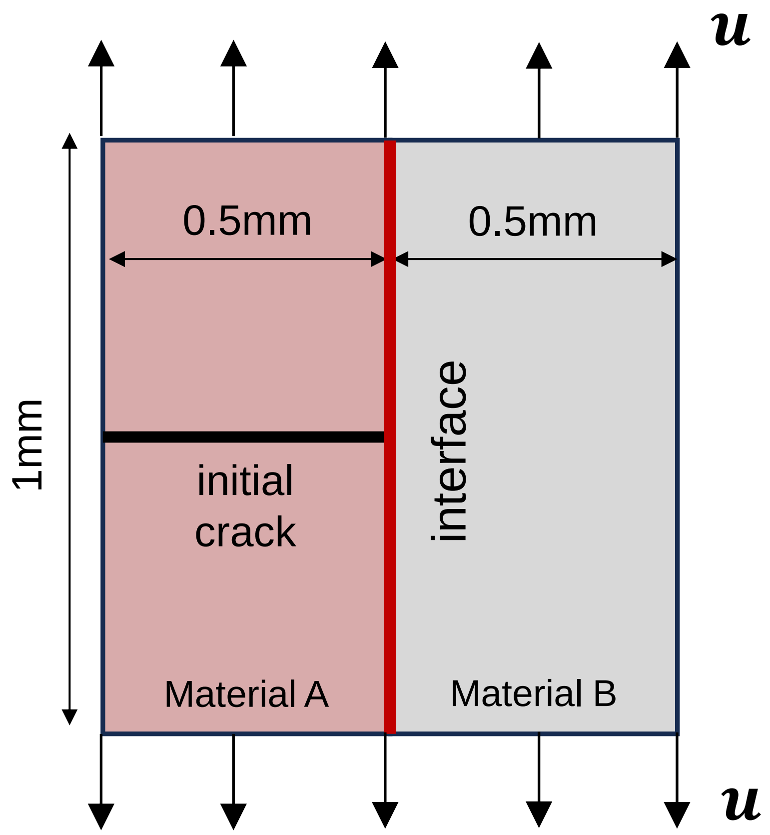

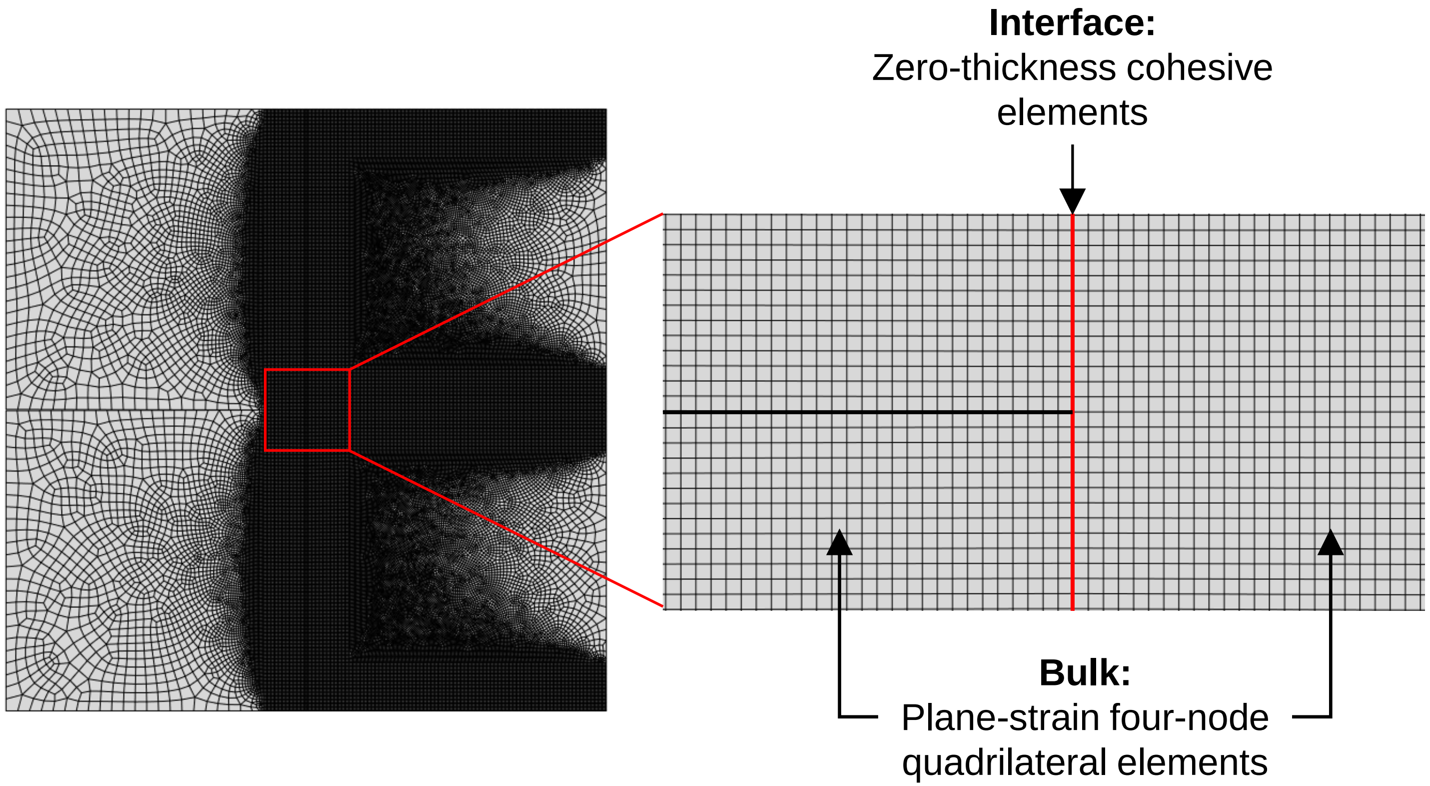

Simulation predictions

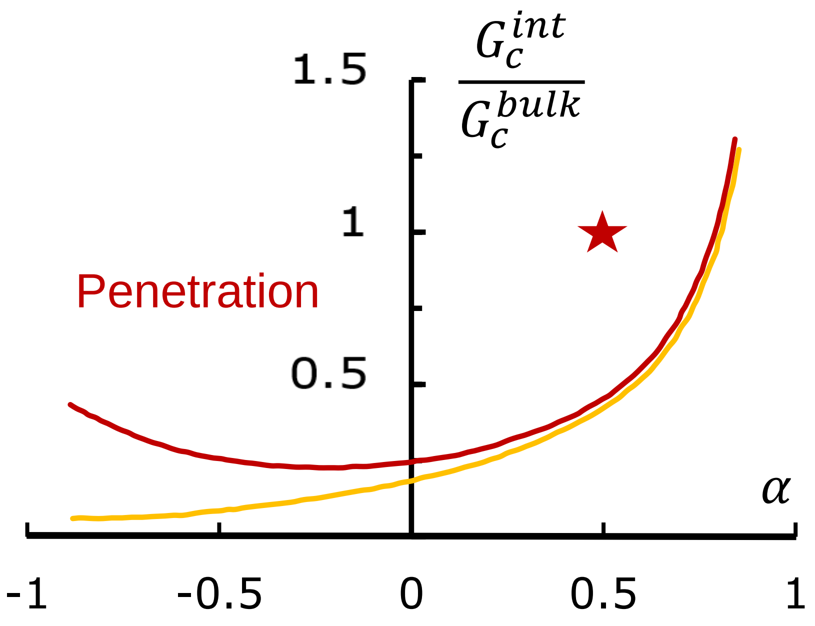

$$\frac{G_c^{int}}{G_c^{bulk}} = 1,\ \alpha = 0.5$$

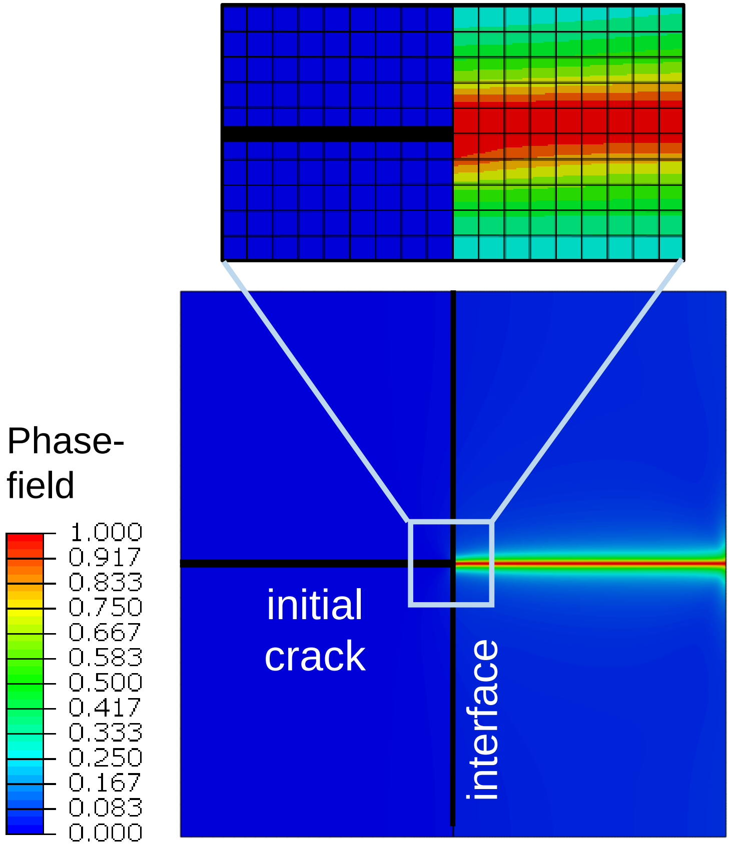

Crack deflection

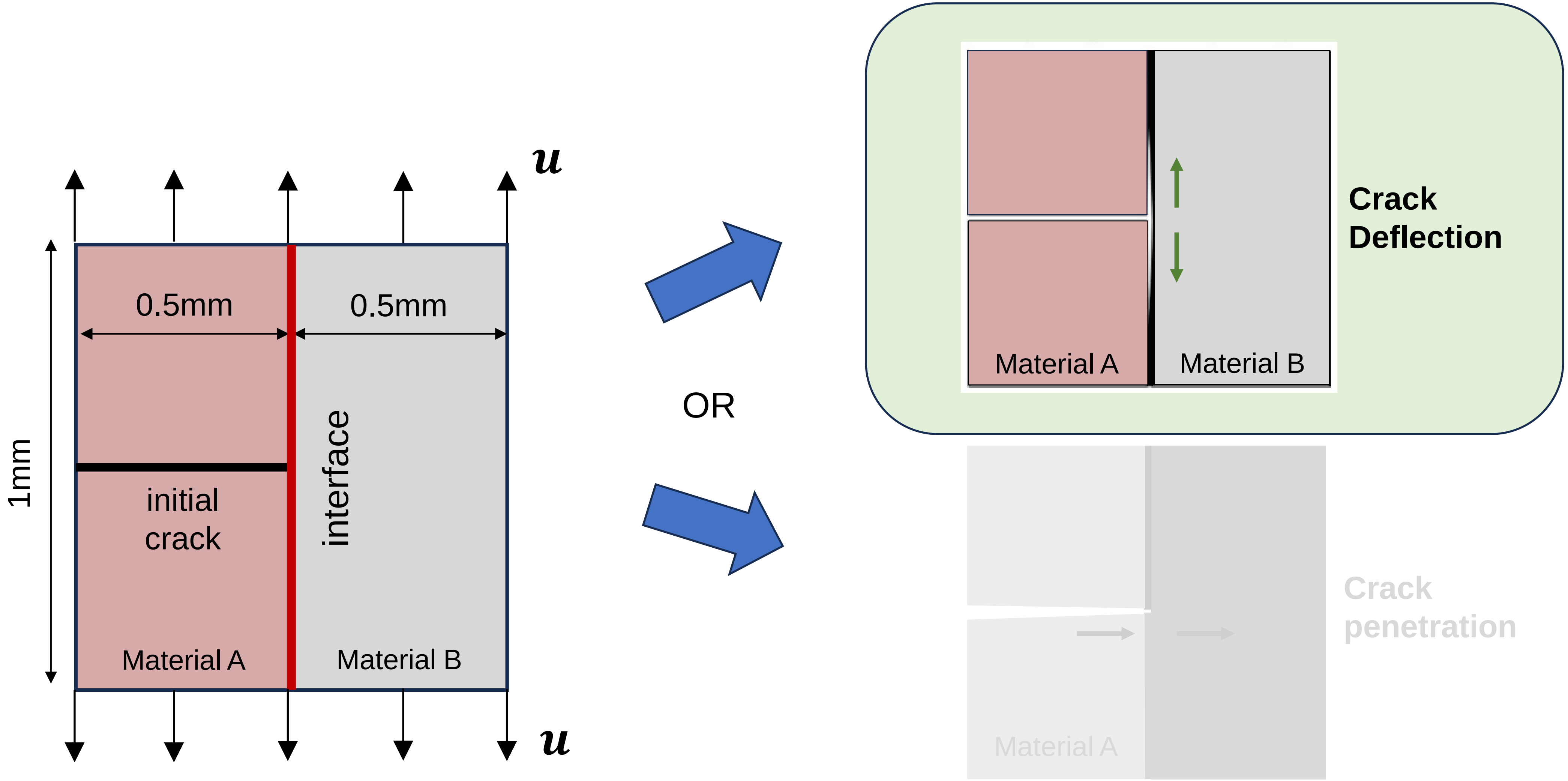

Simulation predictions

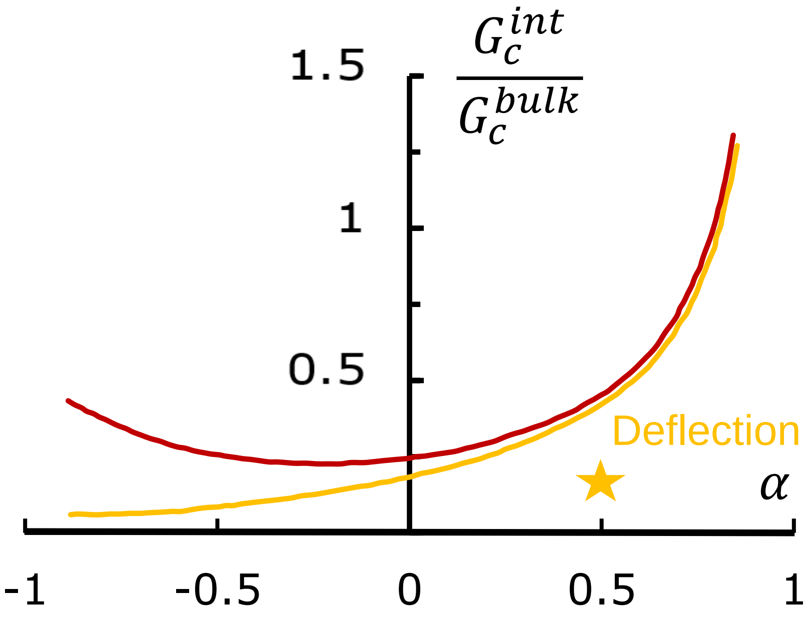

$$\frac{G_c^{int}}{G_c^{bulk}} = 0.2,\ \alpha = 0.5$$

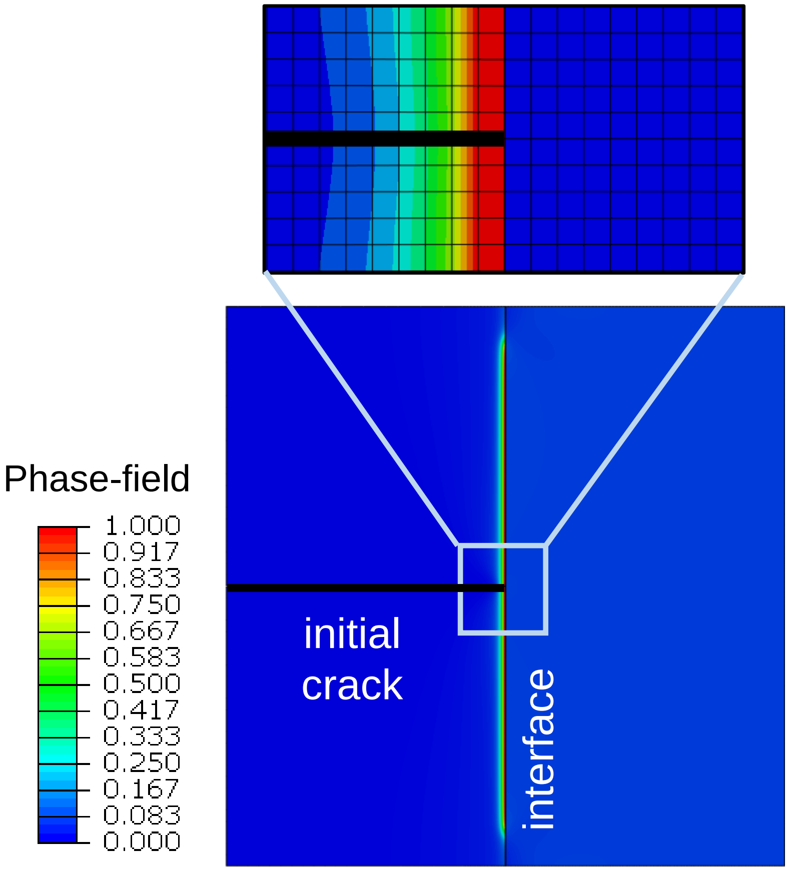

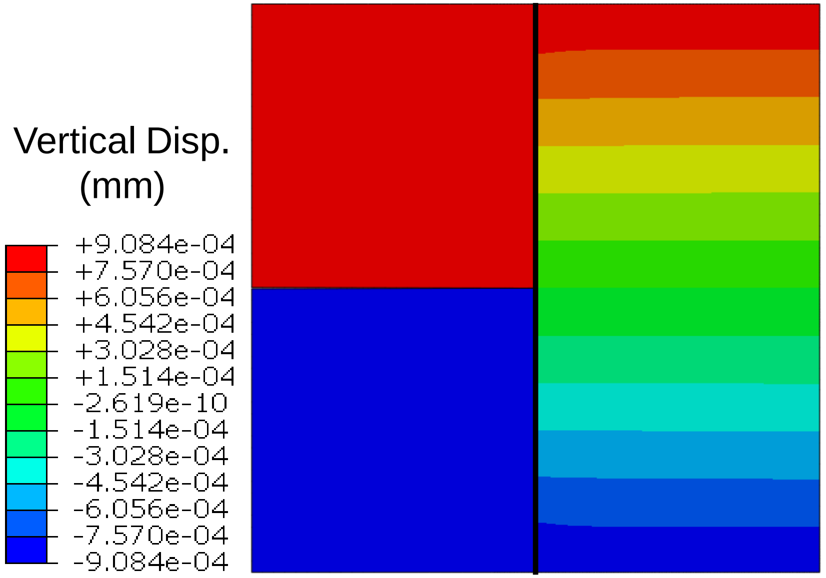

Overall enhanced performance for the case when crack deflects

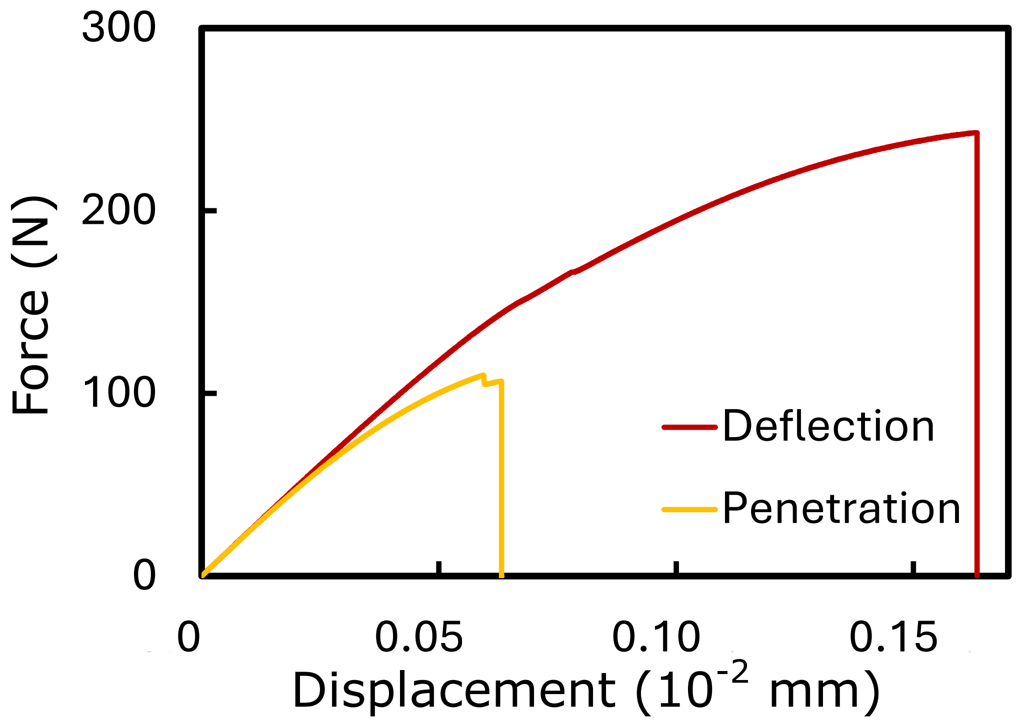

$$\frac{G_c^{int}}{G_c^{bulk}} = 0.2$$
$$\alpha = 0.5$$

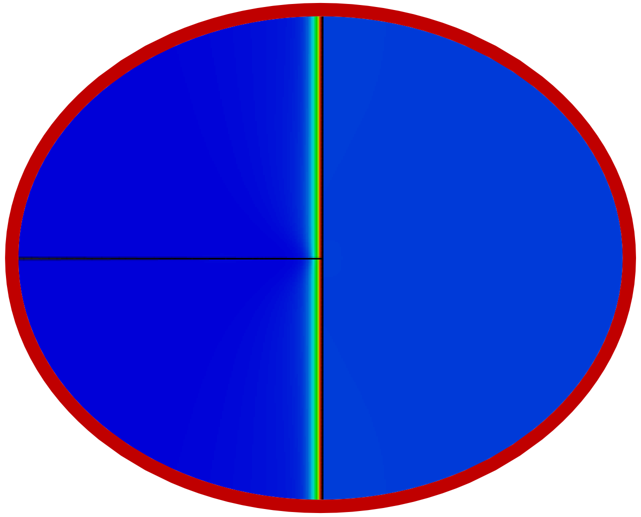

Deflection

$$\frac{G_c^{int}}{G_c^{bulk}} = 1$$
$$\alpha = 0.5$$

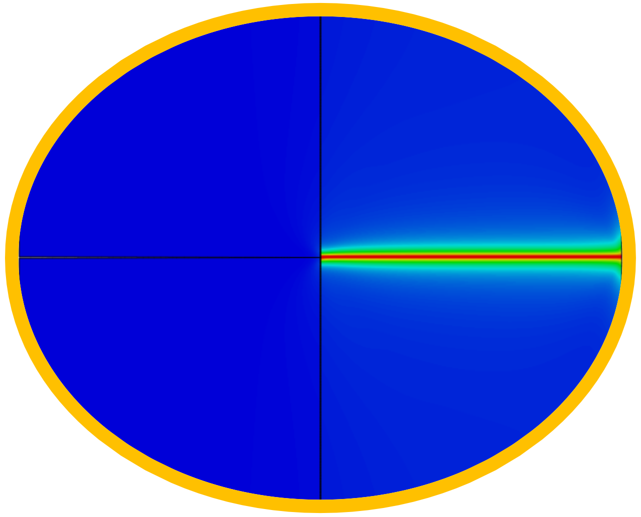

Penetration

Crack impinging on an inclined interface

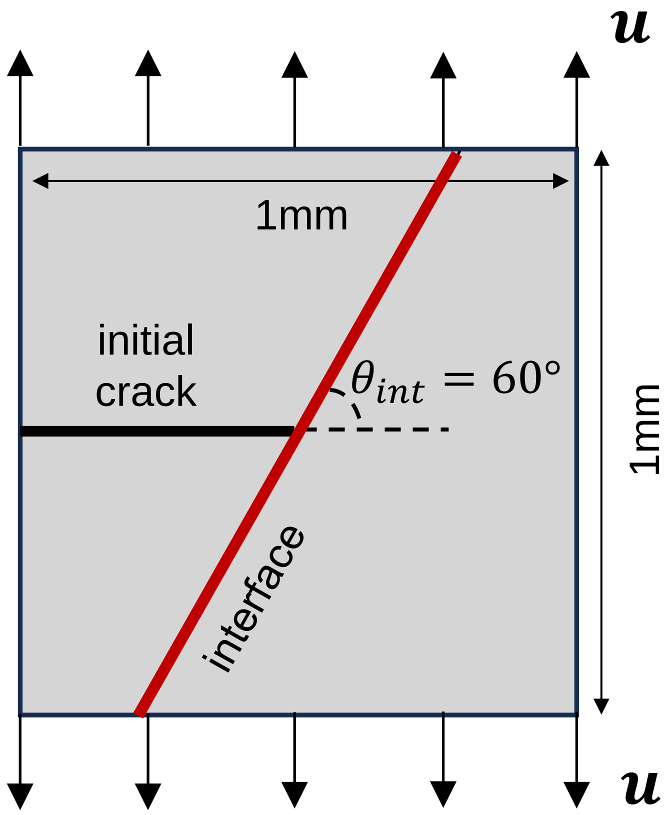

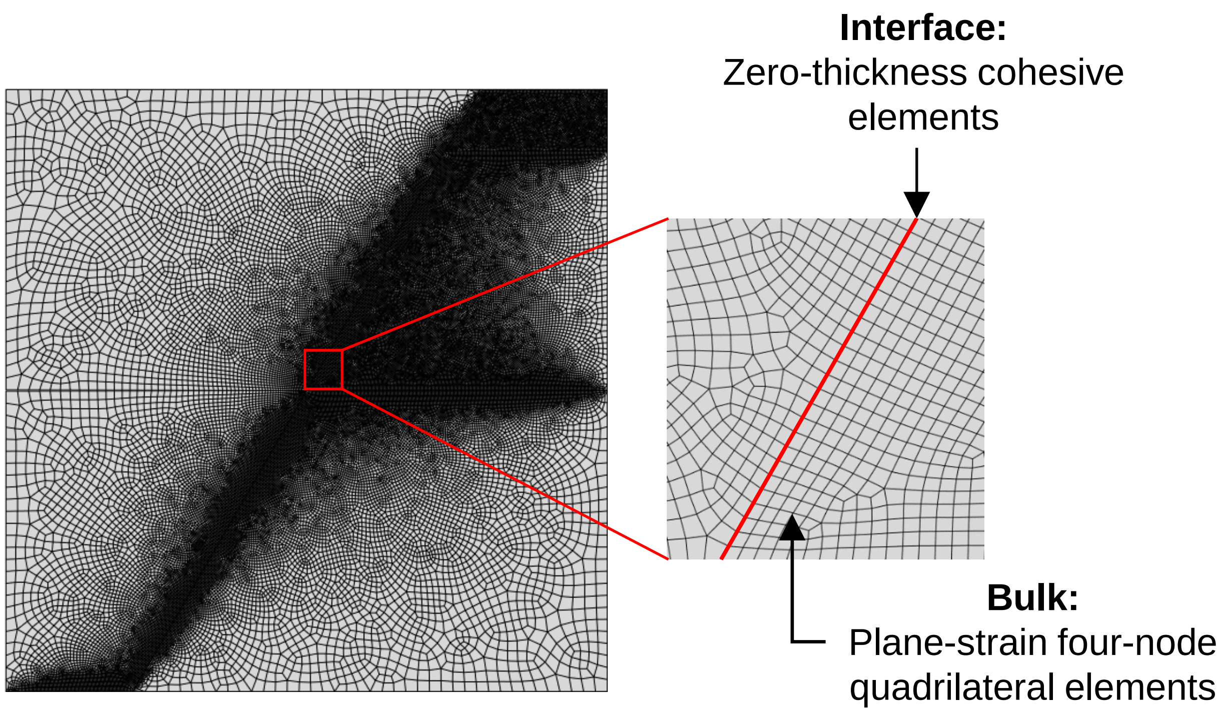

LEFM theory for the case of a crack impinging on an inclined interface [1]

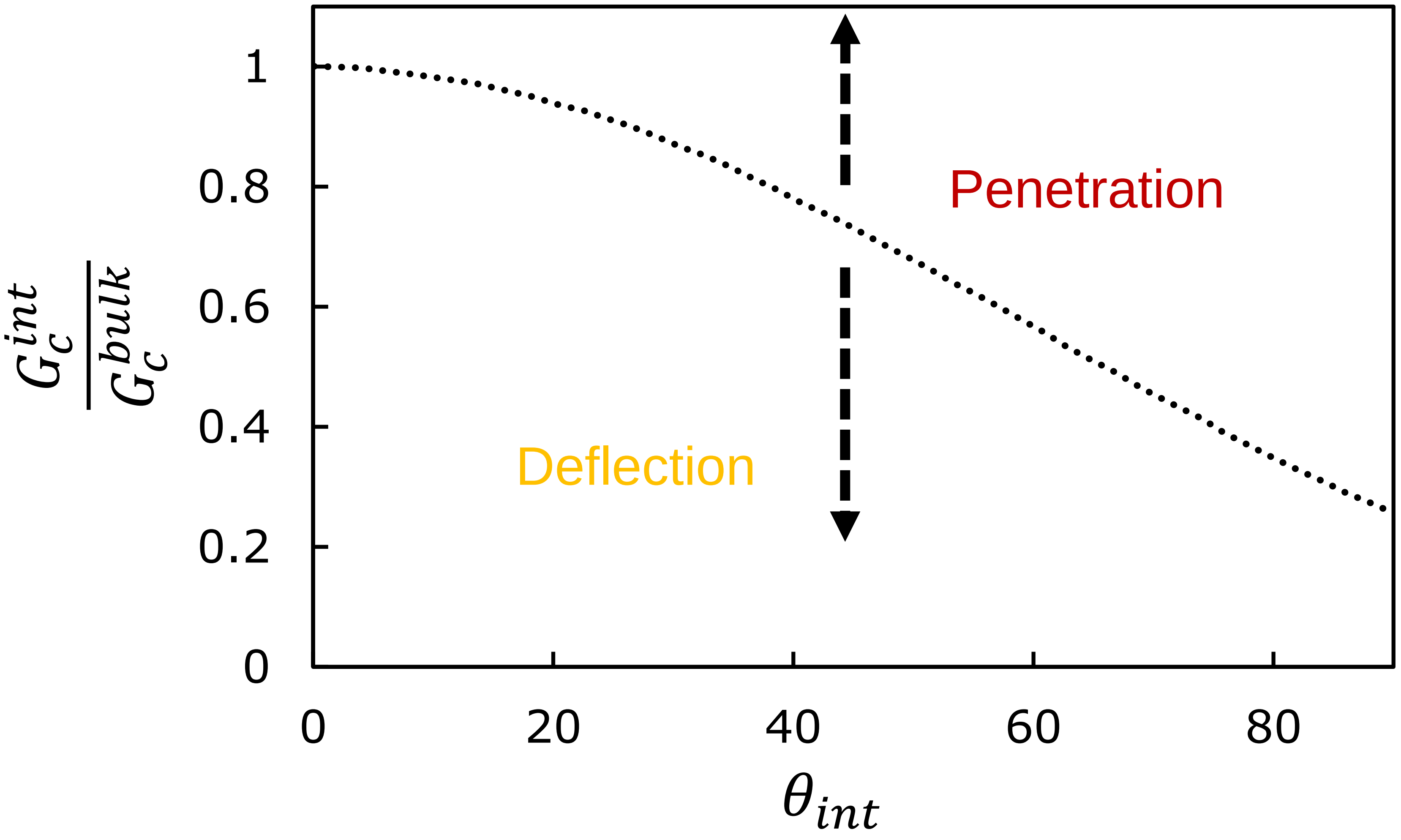

[1] He and Hutchinson / *Int. J. Solids Structures* 29 (1989) 63-191

Framework predictions

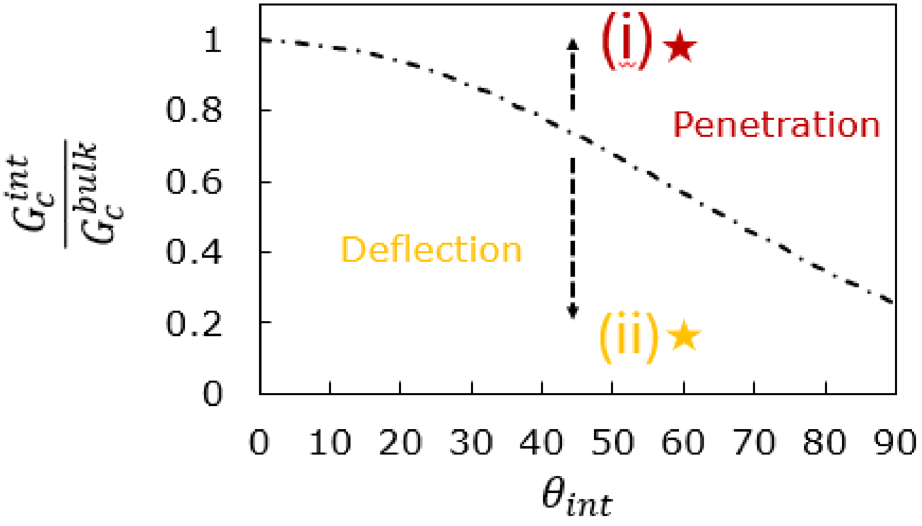

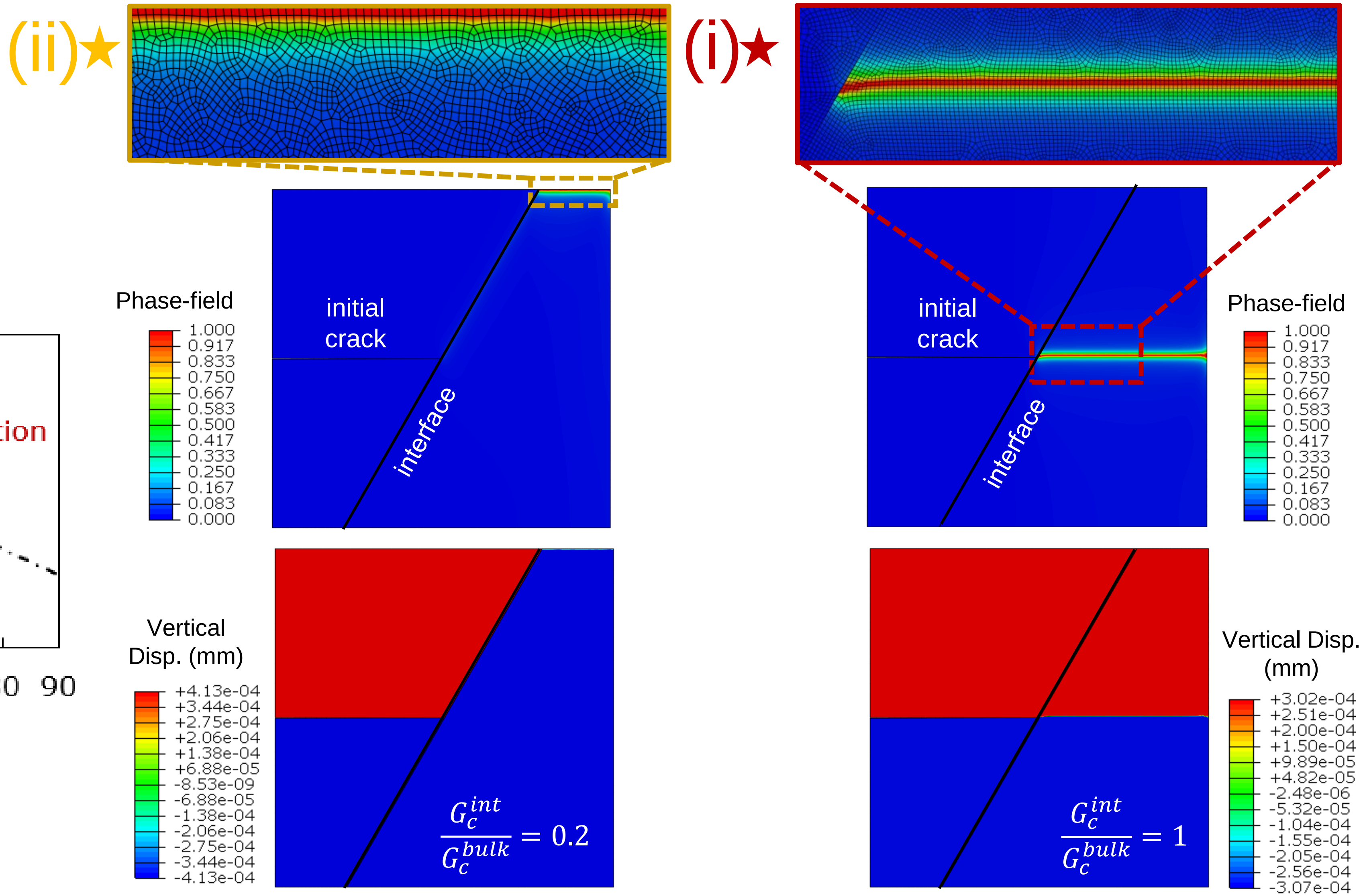

Crack deflection

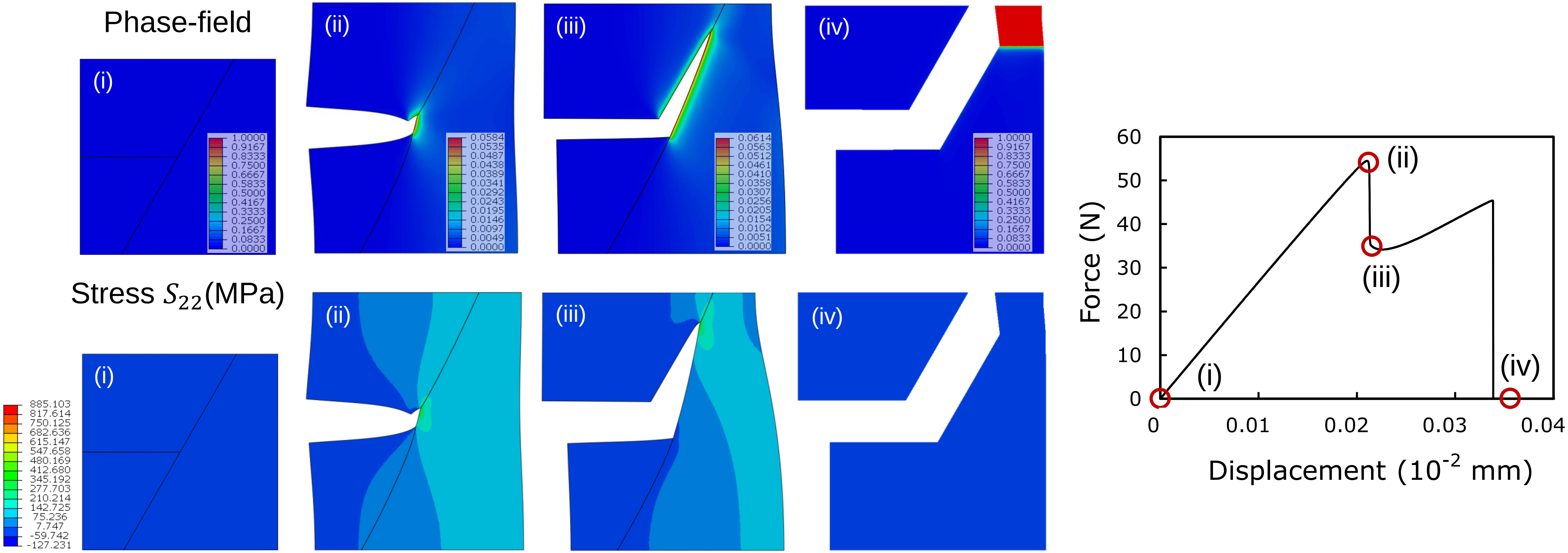

Interface separation is captured

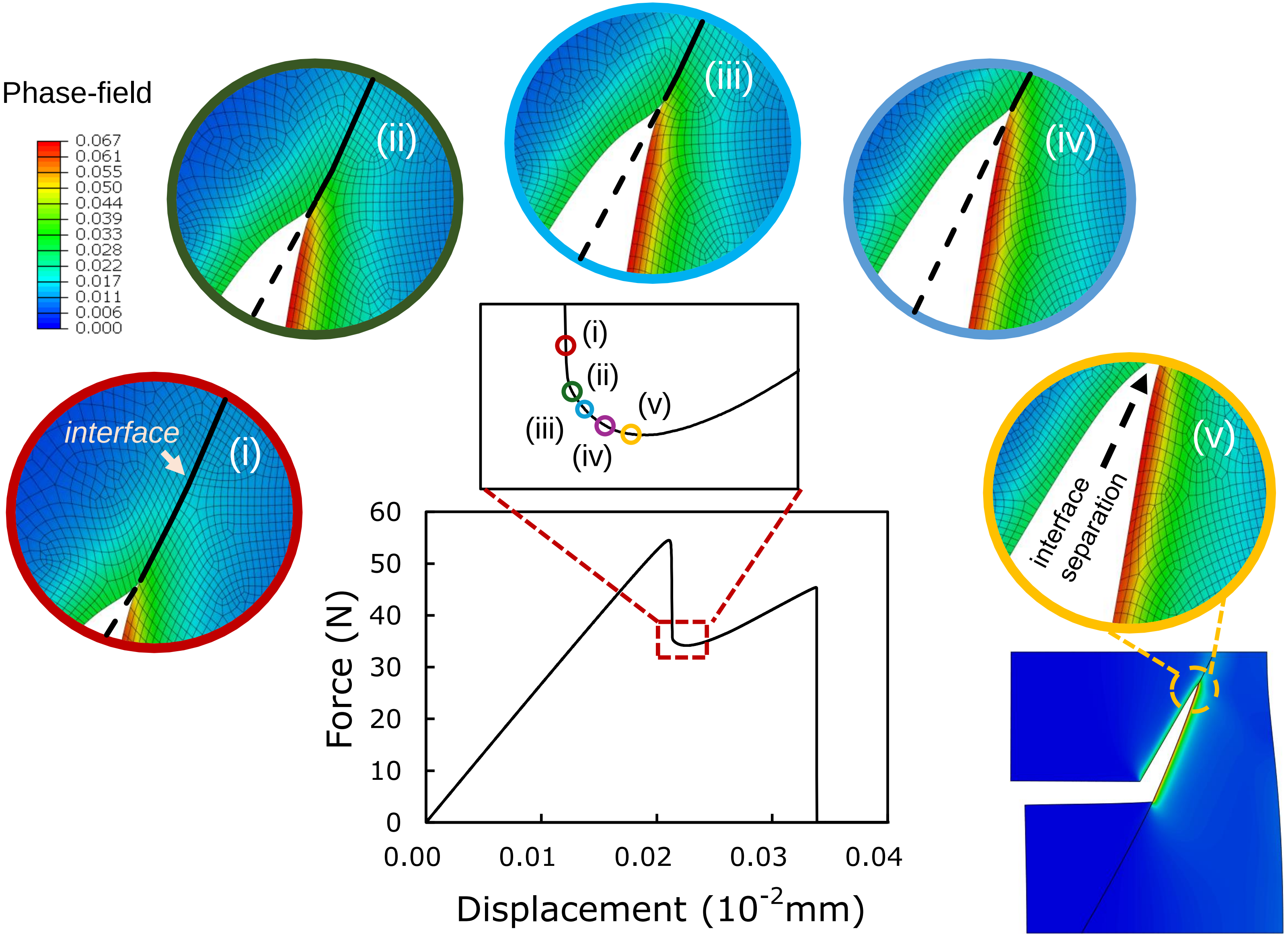

Crack penetration

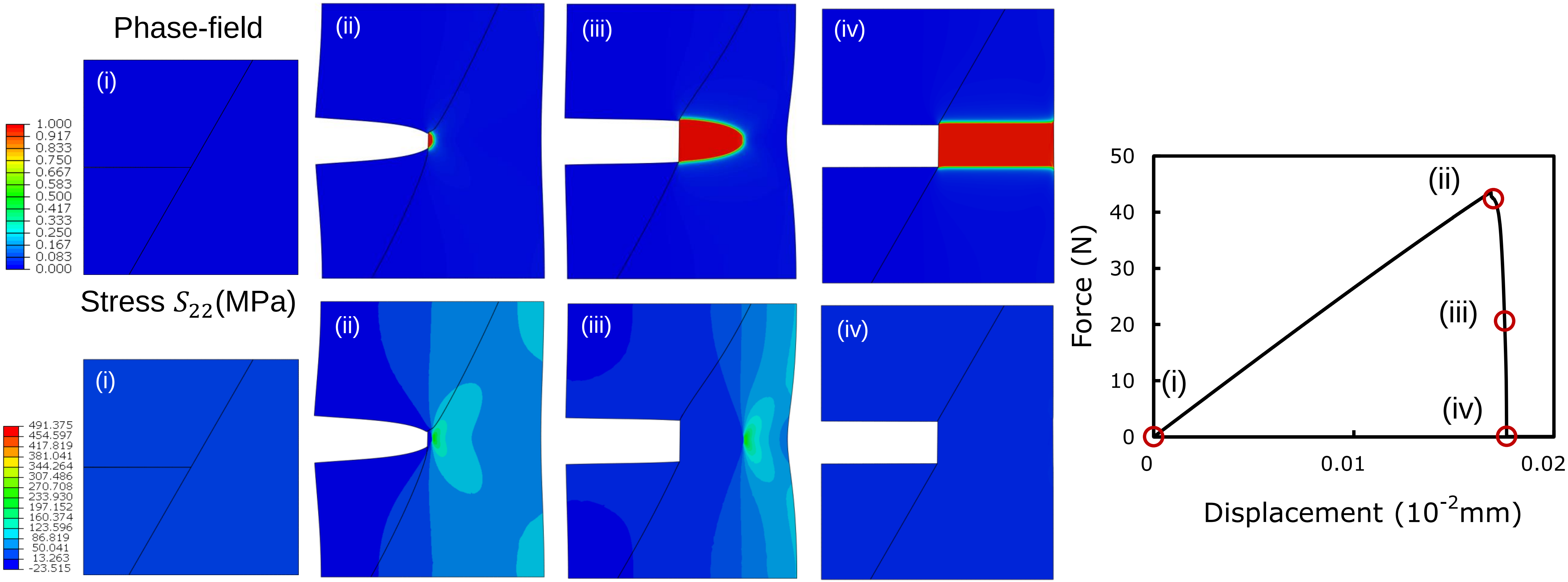

Case III: hard-soft-hard tri-layer composite with interface perpendicular to initial notch direction

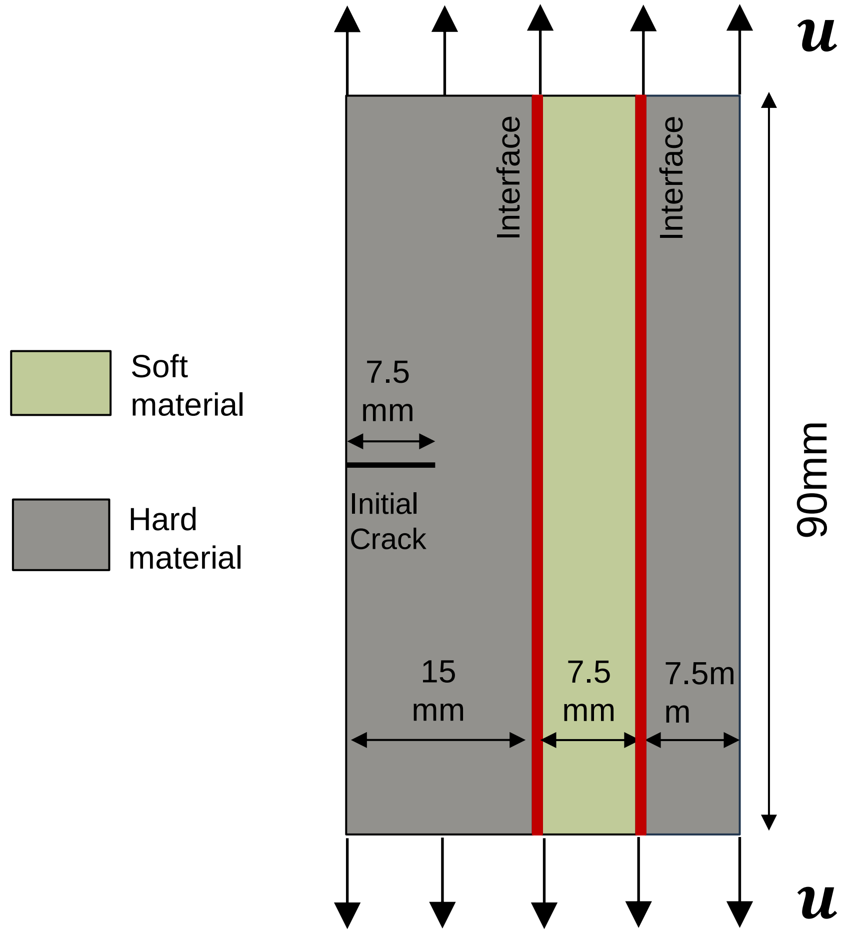

Case IV: fiber-reinforced matrix composite

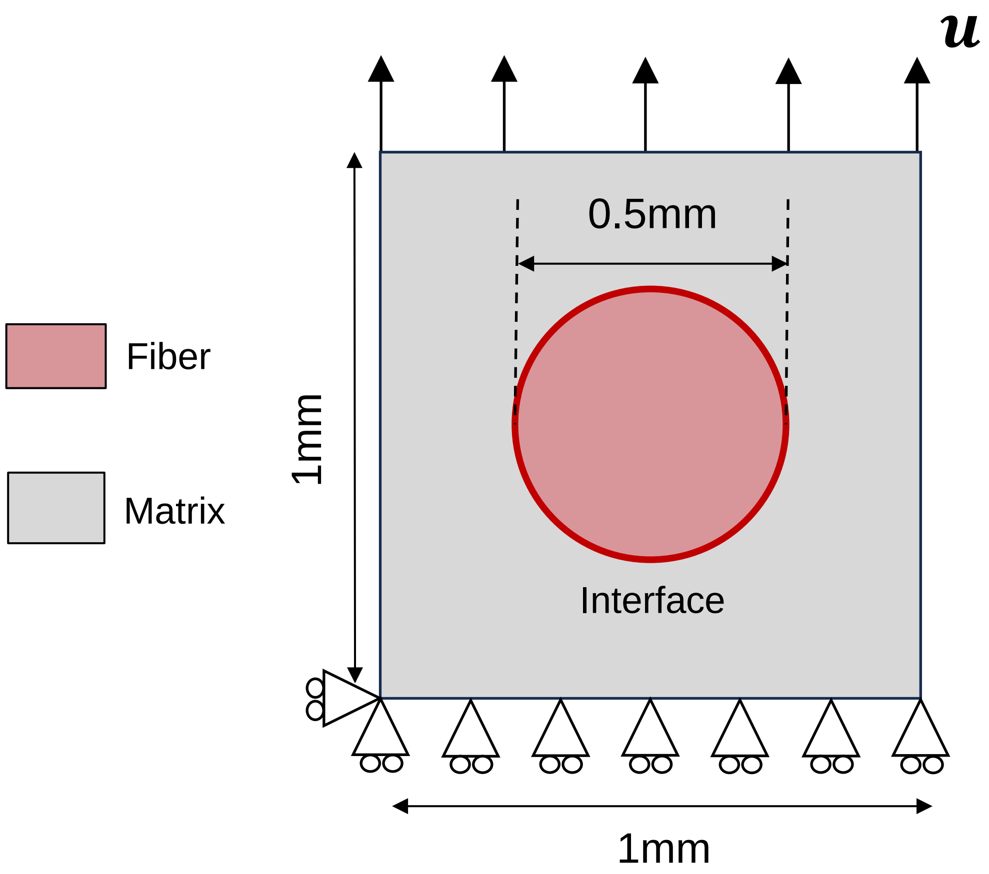

Zero-thickness cohesive elements used for interface - 4-node quadrilateral plane strain elements used for bulk

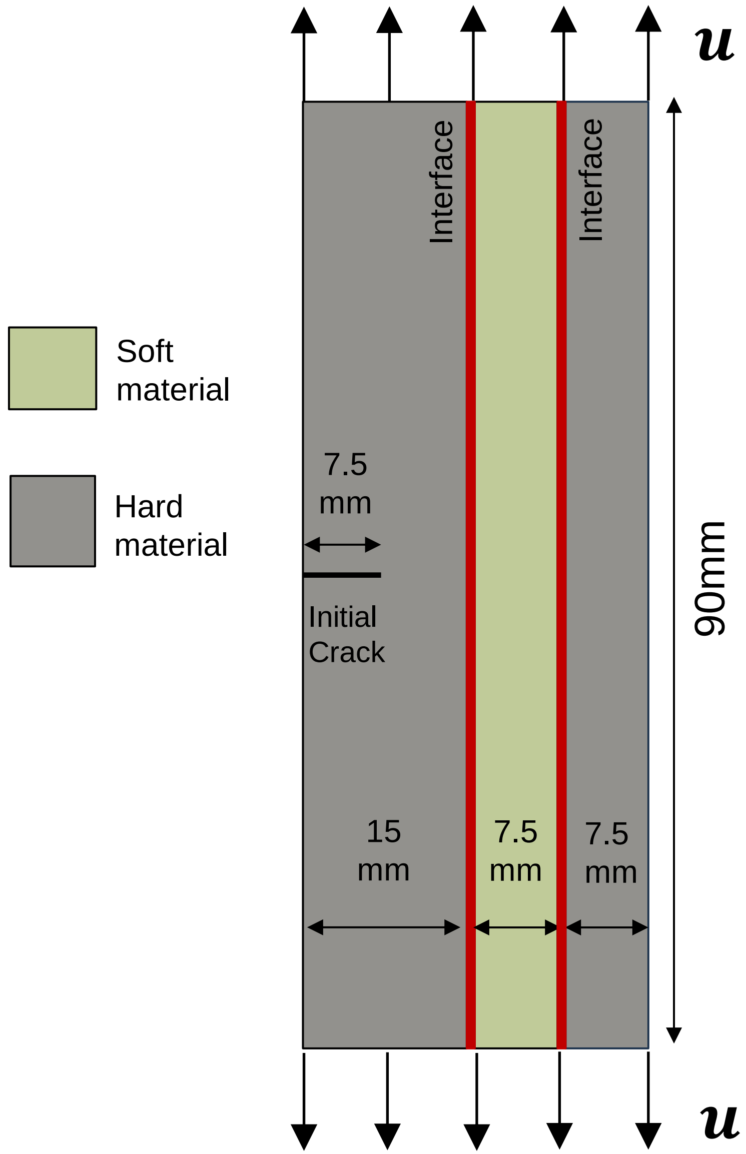

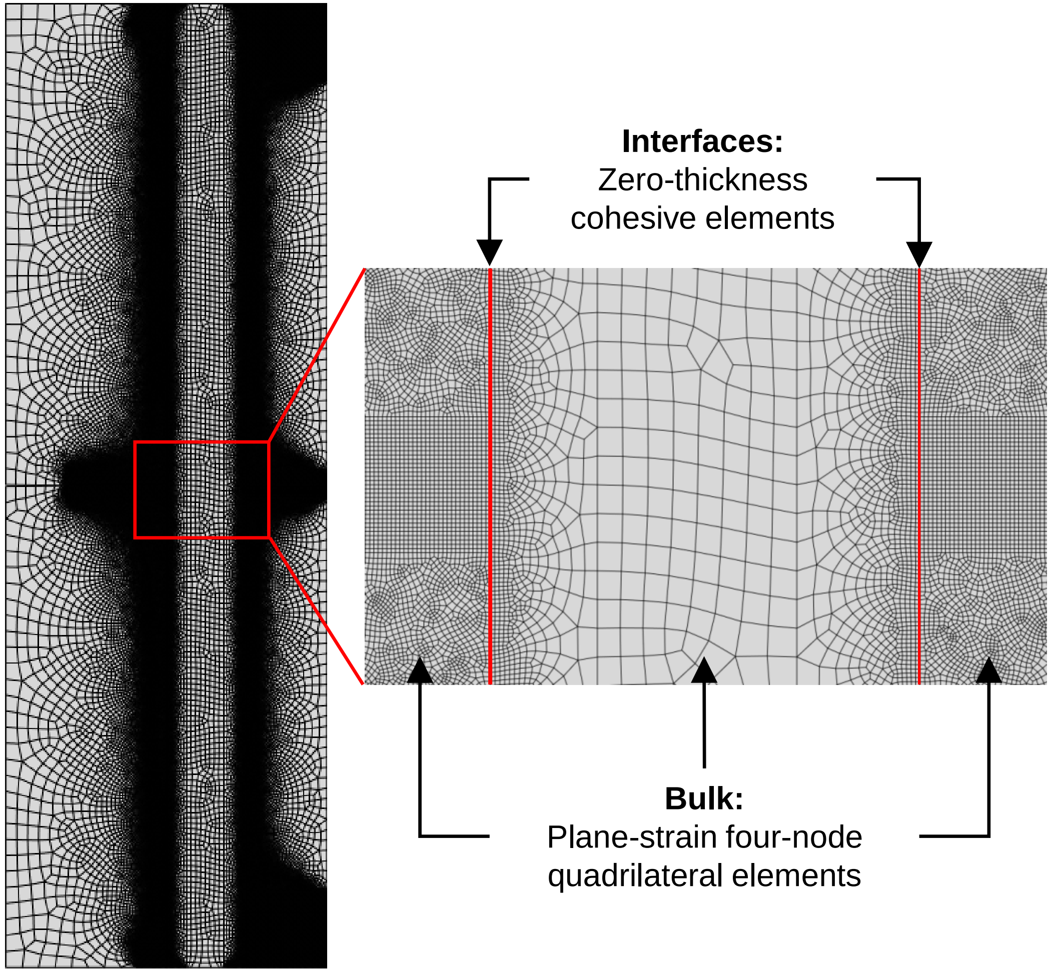

Material properties were determined using specific mechanical characterization tests

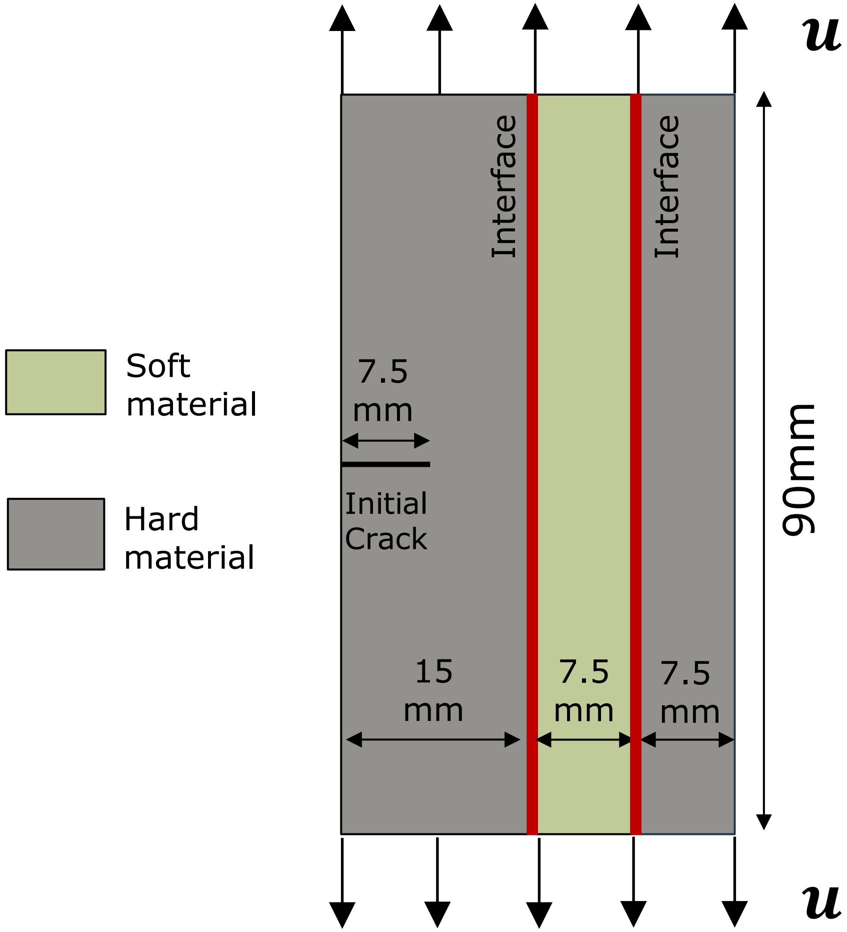

	Hardened Cement Paste	PVS	Interface
Mechanical properties	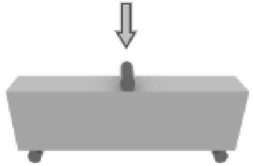 Modulus of rupture σ_c (MPa) = 3.36 Modulus of elasticity[a] E_c (MPa) = $2.2e^4$ Poisson's ratio[a] $\nu_c = 0.22$	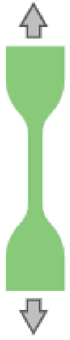 Tensile strength σ_p (MPa) = 1.06 Rubber modulus μ_p (MPa) = 0.4 Poisson's ratio[b] $\nu_p = 0.49$	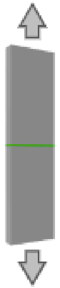 Normal strength σ_n (MPa) = 0.16 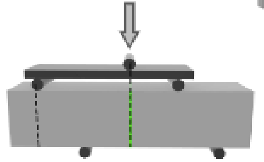 Tangential strength σ_t (MPa) = 0.29
Fracture properties	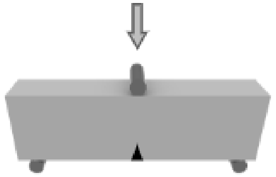 Fracture toughness G_{c_c} (N/mm) = $4.47e^{-3}$	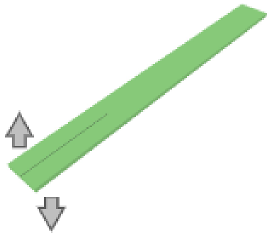 Fracture toughness G_{c_p} (N/mm) = 1.29	Mode-I Fracture toughness G_{c_I} (N/mm) = 1.23 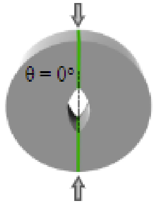 $\theta = 0°$ Mode-II Fracture toughness $G_{c_{II}}$(N/mm) = 1.29 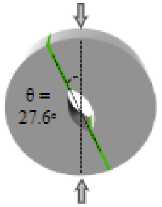 $\theta = 27.6°$

[1] C.-J. Haecker et al. / Cement and Concrete Research 35 (2005) 1948 – 1960

[2] Coulais et al. / Physical Reviews Letters (2015) 115, 044301

[3] Manan et al. / Journal of Engineering Materials and Technology (2021) 143, 041006-3

Crack propagation mechanism in tri-layer hard-soft-hard composite

Phase-field

Stress S_{22} (MPa)

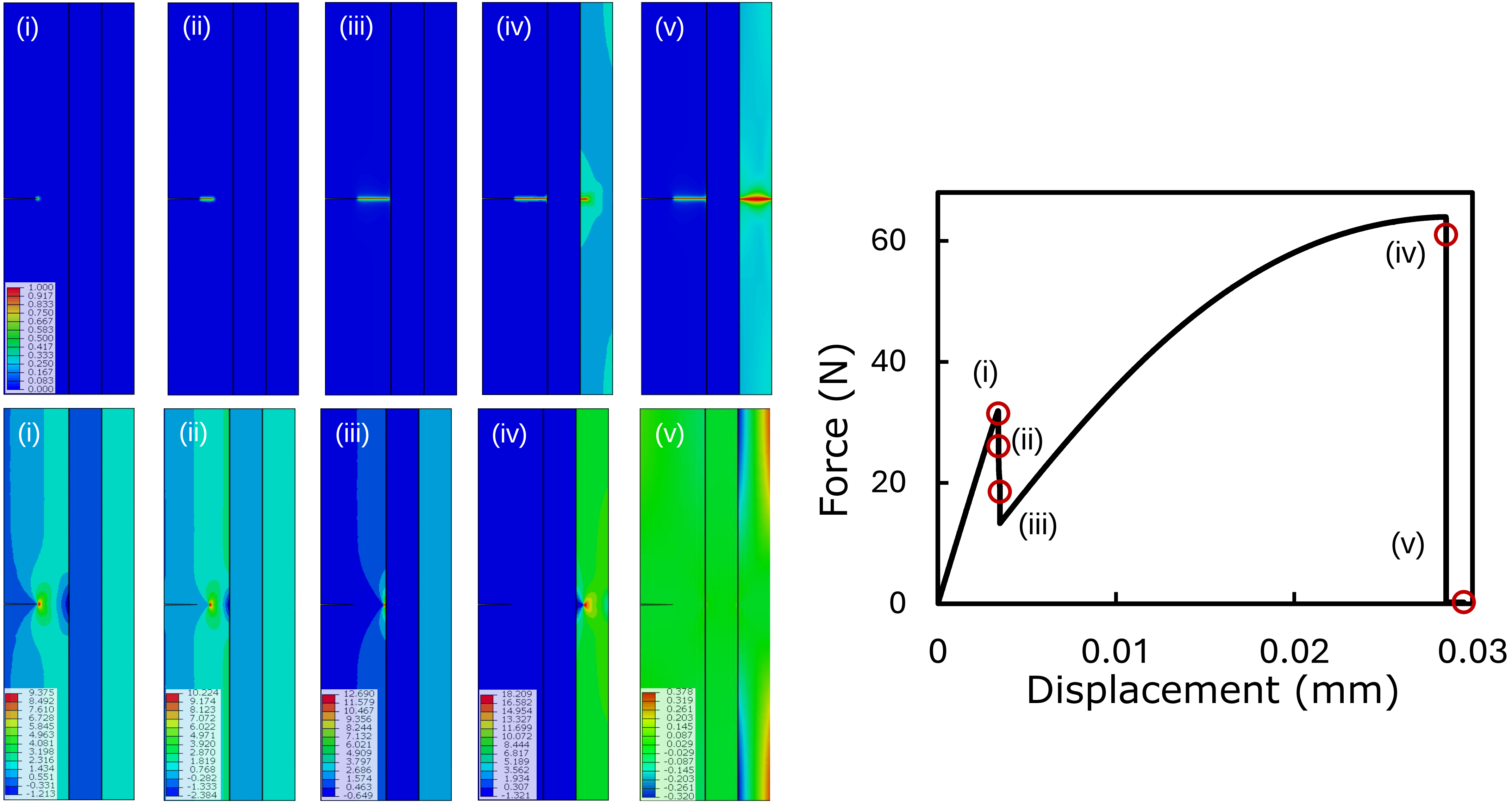

Effect of thickness on overall performance

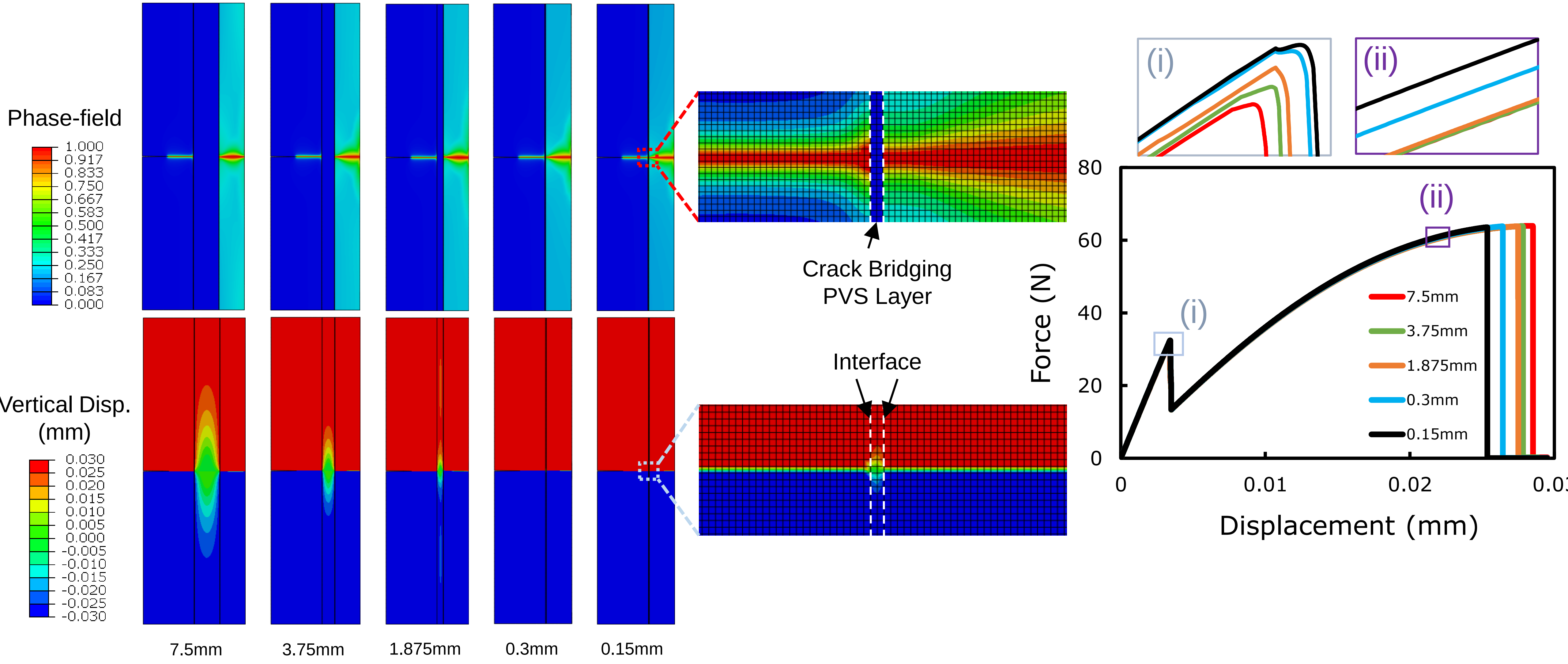

Hardened cement-PVS composite shows significant increase in toughness vs. monolithic

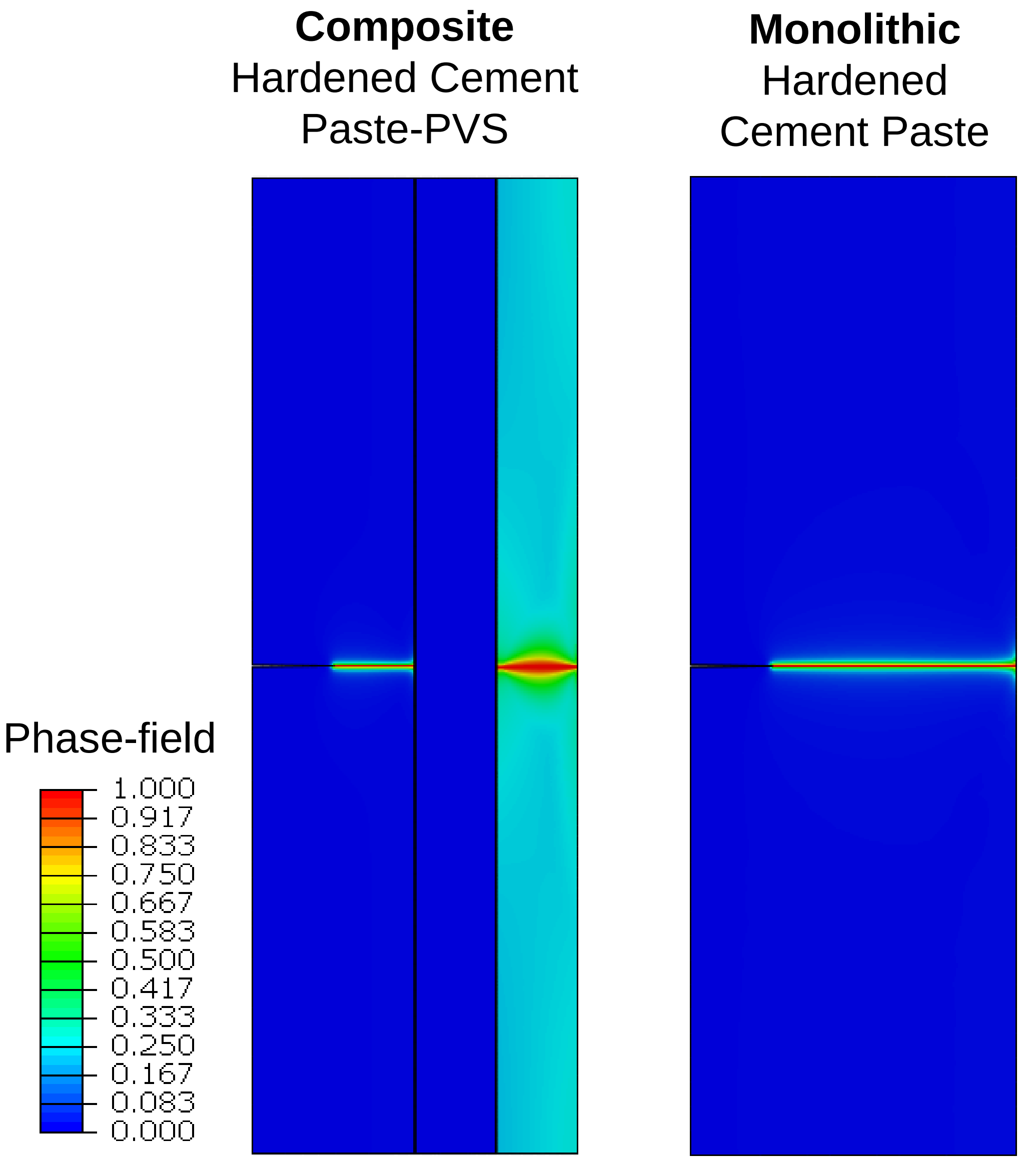

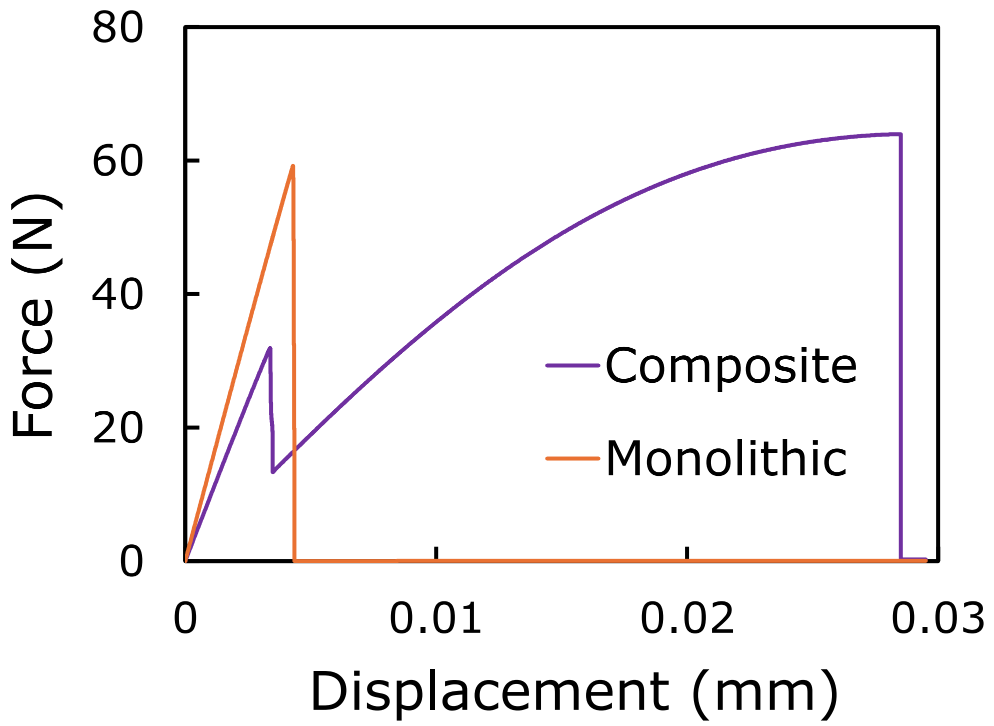

Case I: hard-hard bi-layer composite

To illustrate the capability of the framework in capturing deflection and penetration

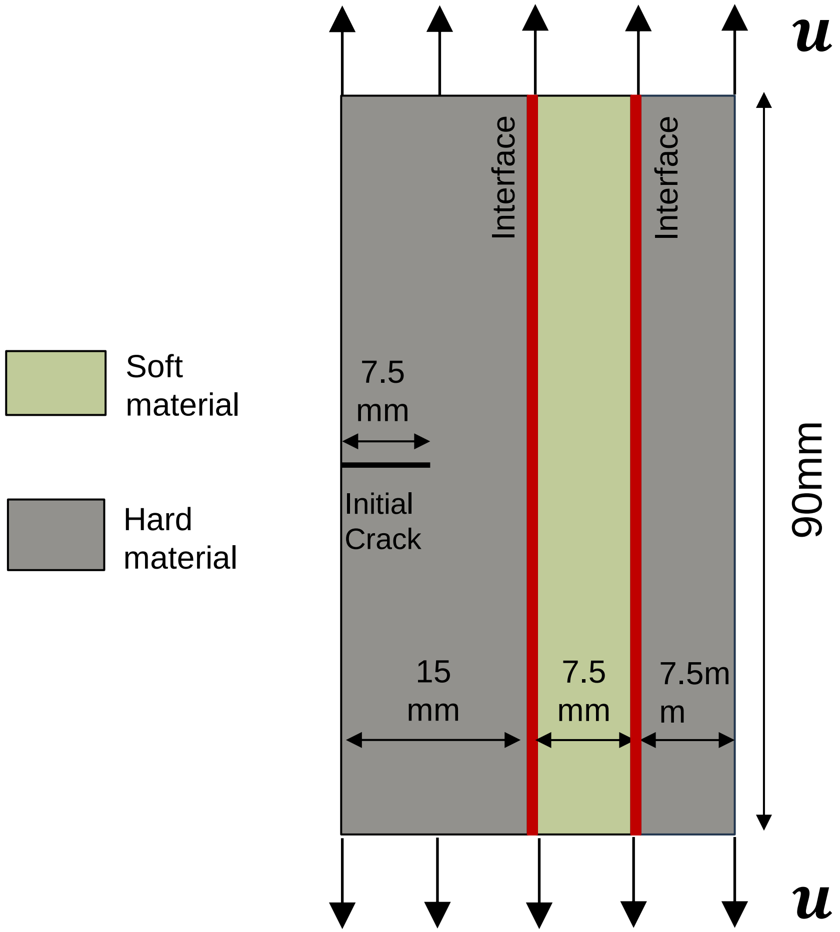

Case II: hard-soft-hard tri-layer composite

To examine toughening mechanisms achieved by exploiting compliancy of soft material

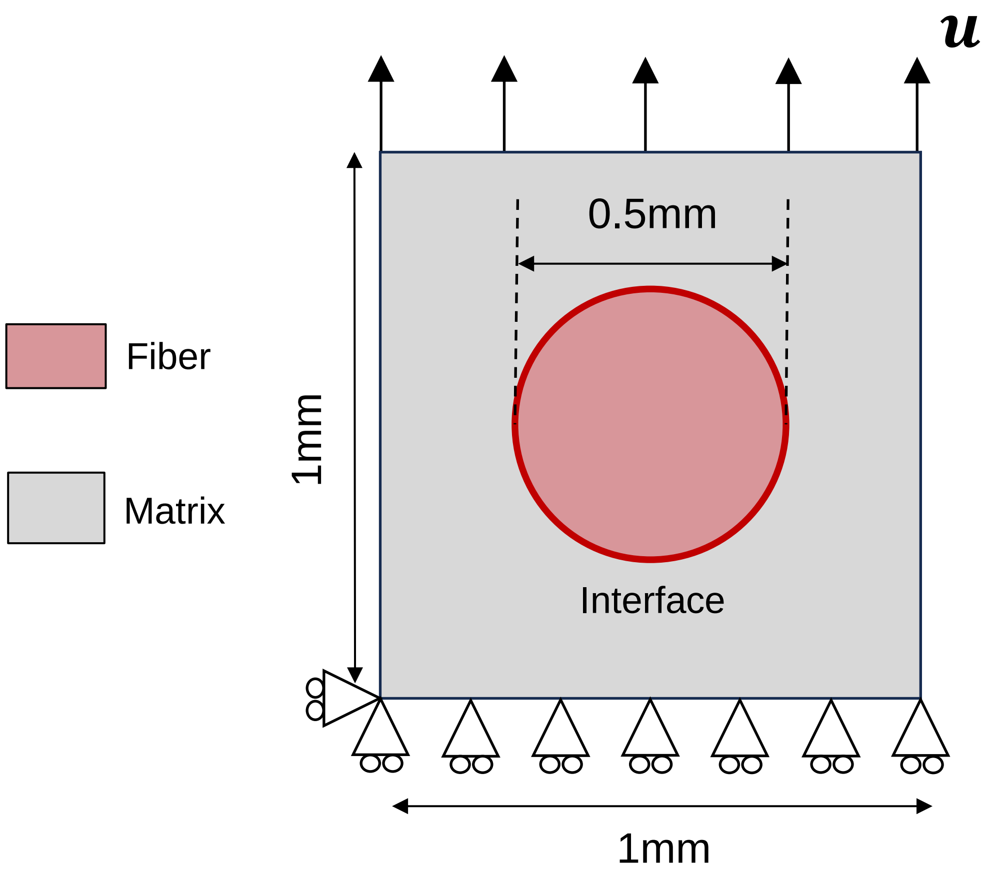

Zero-thickness cohesive elements used for interface - 4-node quadrilateral plane strain elements used for bulk

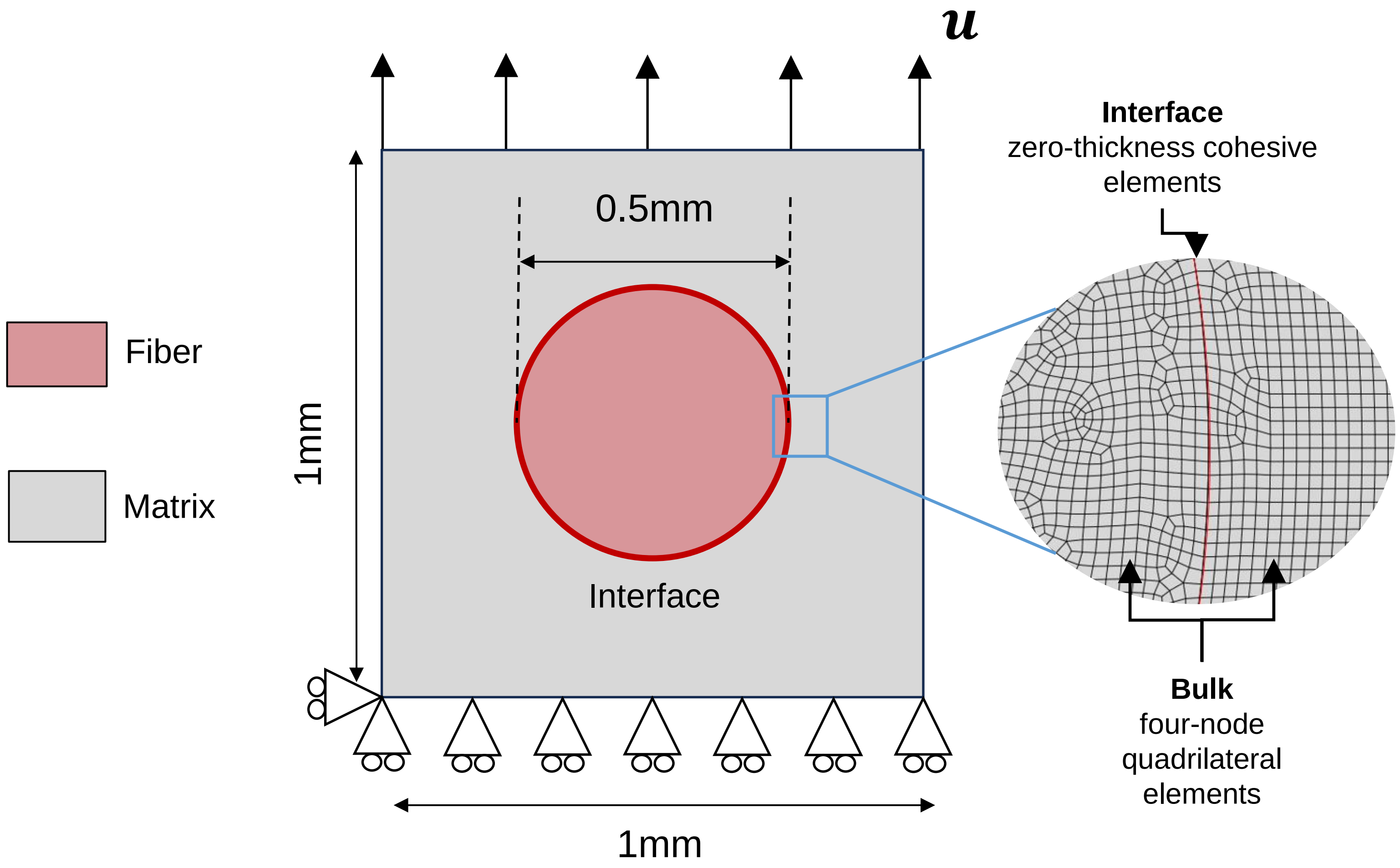

Framework predictions

Stress S_{22} (MPa) Phase-field

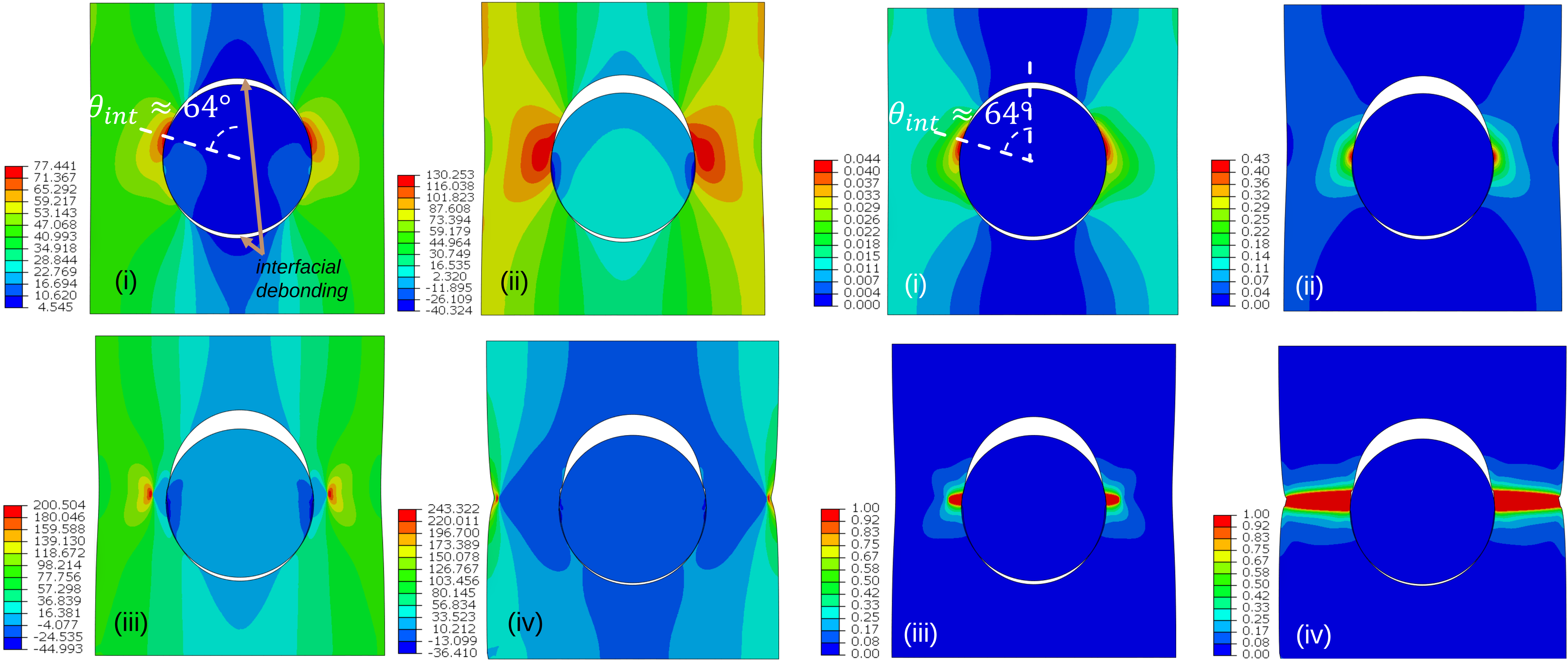

Framework predictions

Phase-field

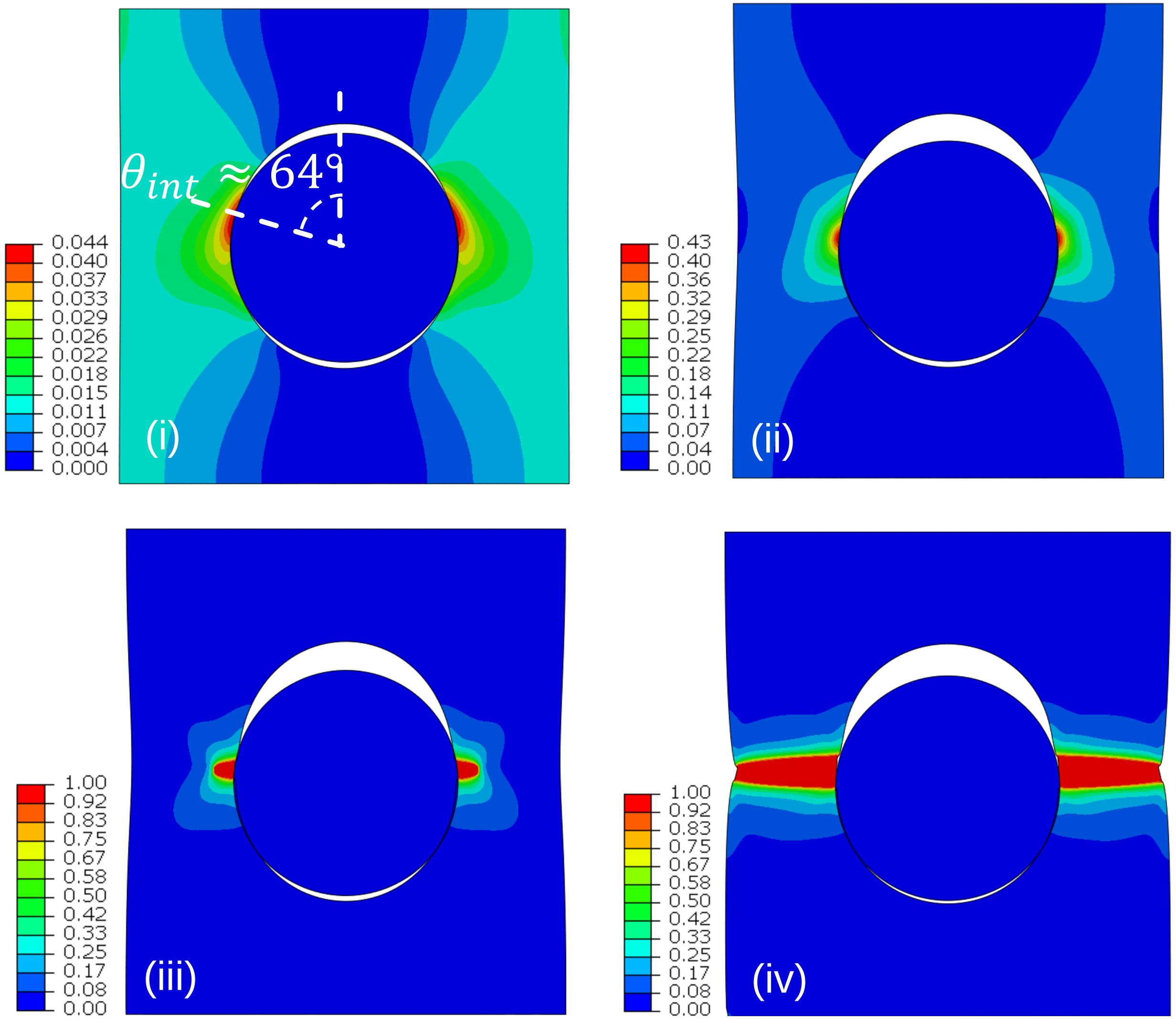

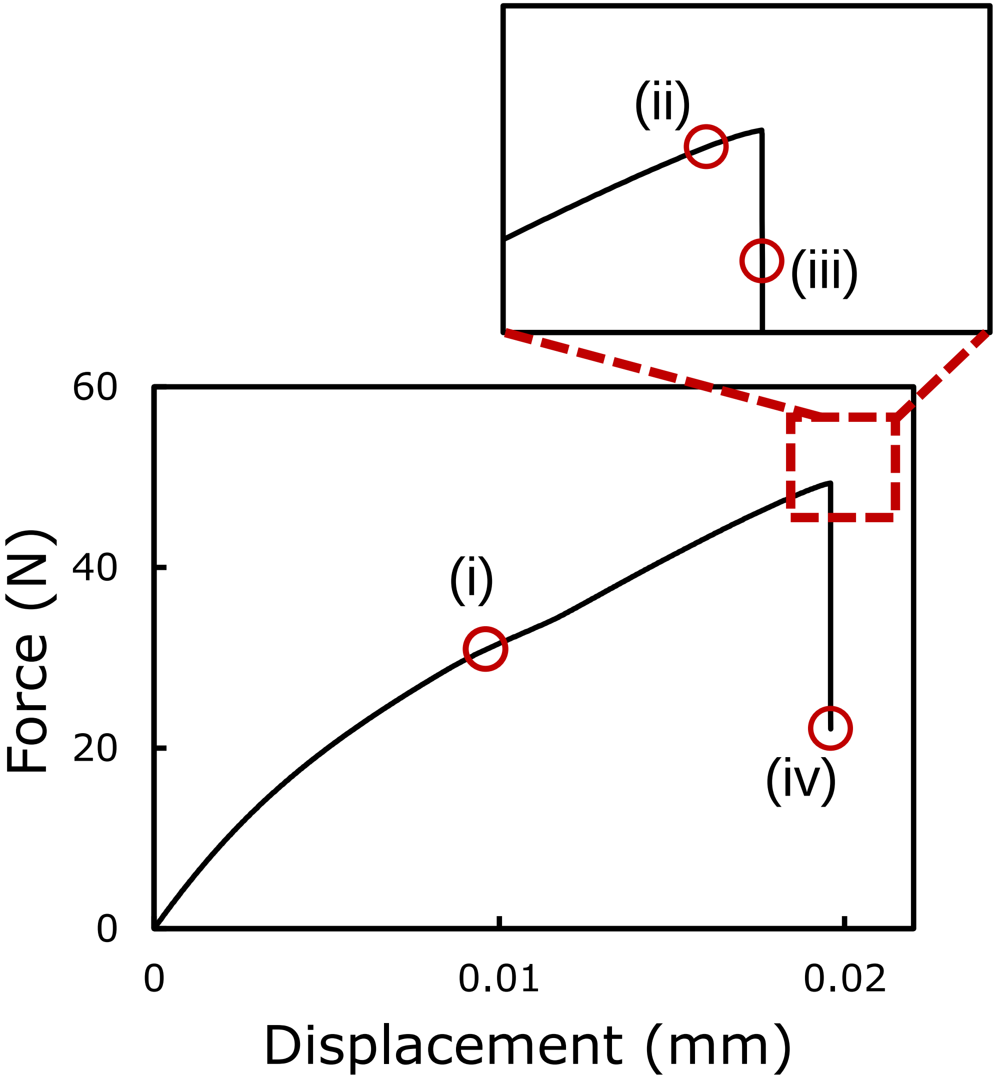

ARCHITECTED MATERIALS AND
ADDITIVE MANUFACTURING LAB

Conclusions

- A unified framework coupling large deformation phase-field and PPR CZM was developed to explore crack growth in hard-hard and hard-soft multi-material systems

- The framework can capture crack deflection and crack penetration in hard-hard composites containing weak interfaces in accordance with predictions of Linear Elastic Fracture Mechanics (LEFM)

- The framework captures an emergent crack growth mechanism in hard-soft (Cement-PVS) composites: crack bridging by the soft layer

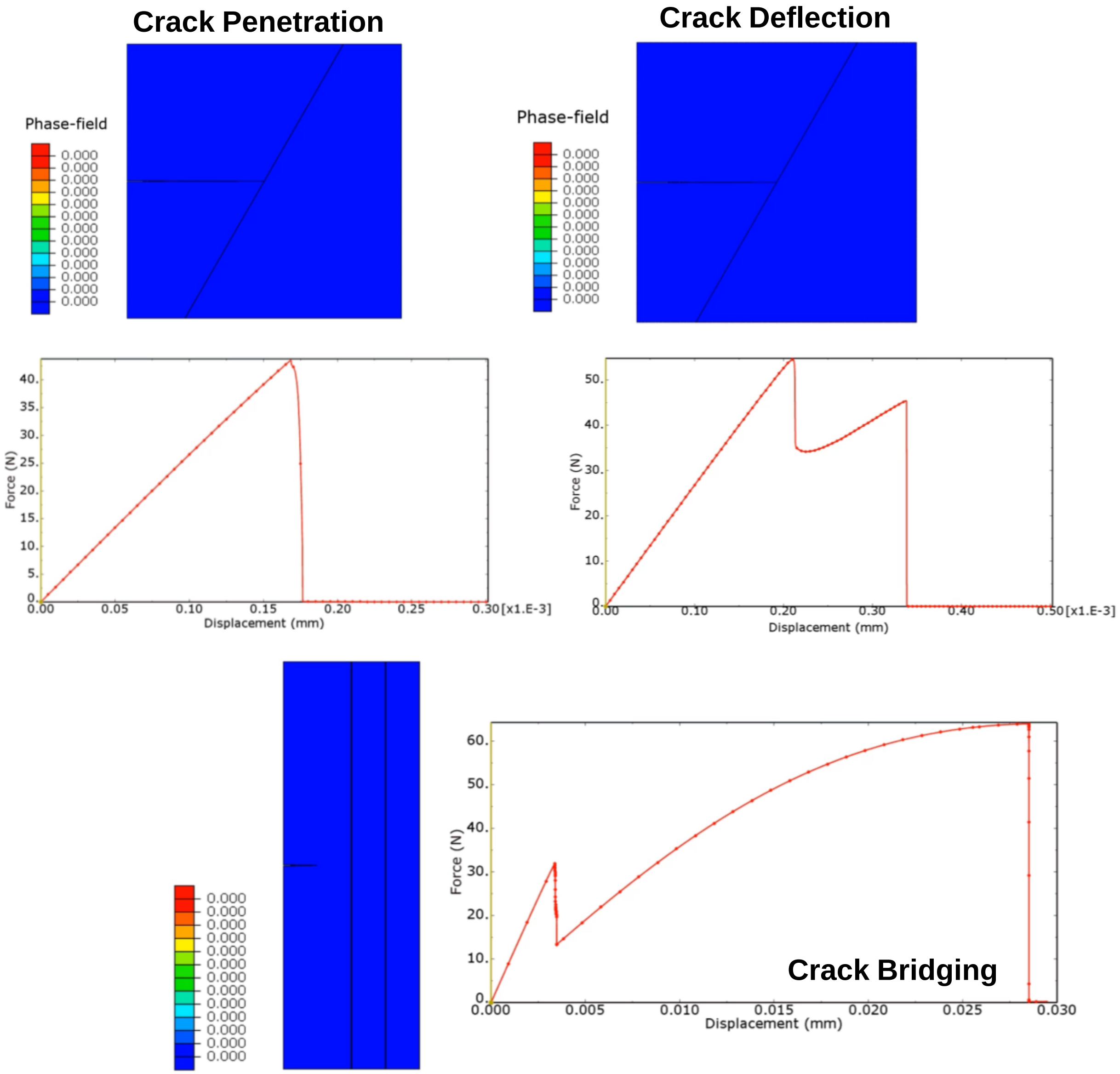

Thank you for your attention! Questions?